Chapter 2

Evaluating Aminoacylation and Suppression Efficiency of Nonsense and Frameshift Suppressor tRNAs *In Vitro*

2.1 Introduction

Site-specific incorporation of unnatural amino acids (UAAs) into proteins biosynthetically is a valuable technique that is seeing increased use (1–4). UAAs are site-specifically incorporated into proteins translated *in vitro* and *in vivo* either by nonsense suppression or frameshift suppression (Figure 2.1). The primary site-specific incorporation technique is known as stop codon (nonsense) suppression and requires a suppressor tRNA, with a modified anticodon, that recognizes the stop codon. The amber stop codon (UAG) is primarily utilized for UAA incorporation (Figure 2.1 A), but the opal stop codon (UGA) has been utilized in eukaryotic cells to incorporate a single UAA (5,6). The suppressor tRNA can be chemically aminoacylated with an UAA (2,3,7–9) or enzymatically aminoacylated with an UAA using tRNA/aminoacyl-synthetase pairs (4,5,10,11). Currently over 100 UAAs or residues (five times greater than the 20 naturally occurring amino acids (aas)) have been incorporated by chemically aminoacylated tRNAs (12), but at the onset of this research only a single UAA could be incorporated into a protein.

The Dougherty group uses nonsense suppression of the amber codon (UAG) to incorporate a single UAA to probe a wide array of structural and functional properties of the mouse muscle nicotinic acetylcholine receptor (nAChR) *in vivo* (2,13–15). A modified *Tetrahymena thermophila* $tRNA^{Gln}$, containing the mutation U73G and the CUA anticodon, (THG73) (16) is chemically aminoacylated *in vitro* with an UAA and injected into *Xenopus* oocytes with ion channel mRNA (with the stop codon, UAG, at the suppression site). To obtain full-length protein, the UAA must be incorporated at the

amber codon or the protein is truncated (Figure 2.1 A) (16). This technique has also been extended to incorporate UAAs in mammalian cells using THG73 (13).

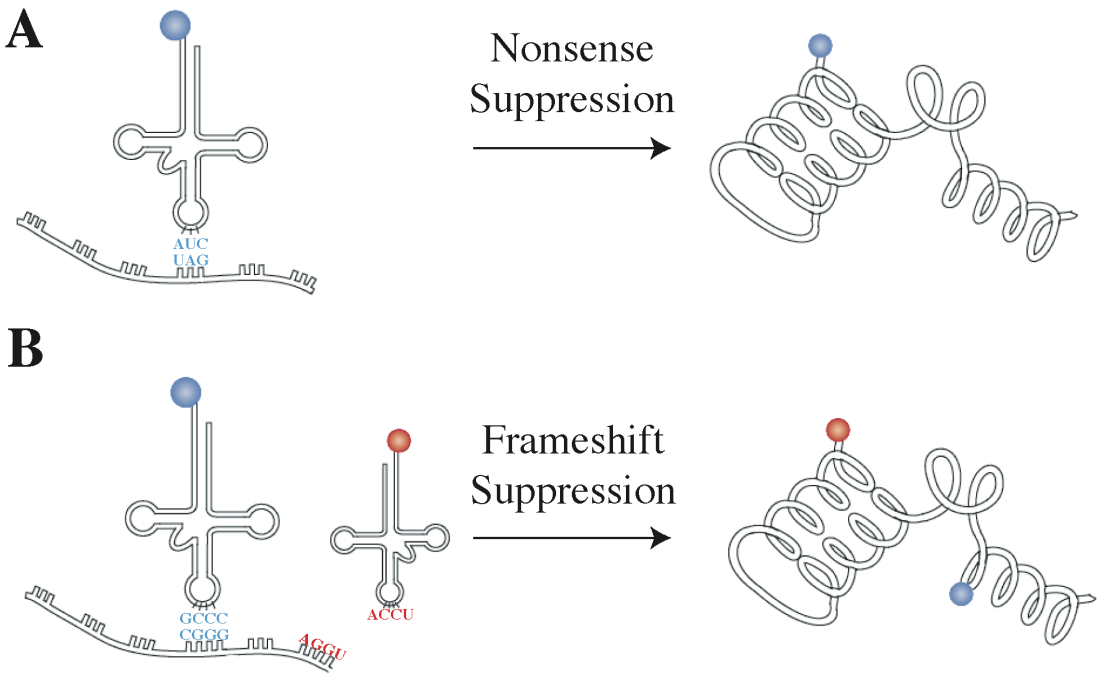

Figure 2.1: UAA incorporation techniques. (A) Nonsense suppression: a stop codon recognizing tRNA suppresses a stop codon and incorporates an UAA. (B) Frameshift suppression: a frameshift suppressor tRNA recognizes a quadruplet codon and incorporates an UAA. Initially this was the only technique that could incorporate multiple UAAs *in vitro* (17). Figure adapted from (1).

Pioneering work developed by Sisido and coworkers used quadruplet codons to incorporate UAAs, which is a technique known as frameshift suppression (18). Using two unique quadruplet codons allowed for the simultaneous incorporation of two UAAs into a single protein translated *in vitro* (17) (Figure 2.1 B). The technique was viable in prokaryotic (18,19) and eukaryotic (20,21) *in vitro* translation systems. Intriguingly, five-base codons could also be utilized to incorporate UAAs, but the suppression efficiency was much less than with four-base codons (22). However, frameshift

suppression was limited to *in vitro* translation systems and *in vivo* UAA incorporation by frameshift suppression had not been shown at the start of this project.

While a single UAA incorporation allows for many useful structure-function studies, incorporation of multiple UAAs would allow for a more diverse experiments; including FRET pairs (23), fluorescence quenching (24), unnatural sulfur derivatives for disulfide cross-linking, and alteration of the sterics and electrostatic properties of more than one amino acid within a protein. Frameshift suppression allows for the incorporation of multiple UAAs *in vitro*, either through the use of two four-base codons (17,24) (Figure 2.1 B) or through the use of one quadruplet codon and the amber codon (UAG) (23,25). These UAA incorporation experiments are typically performed on small, cytoplasmic proteins, such as streptavidin, and it was therefore unknown if large, multi-subunit proteins, such as ion channels, would be feasible for multiple UAA incorporation *in vivo*.

The mechanism of nonsense and frameshift suppression is shown in Figure 2.2. UAA incorporation by nonsense suppression is performed by a tRNA aminoacylated with an UAA that recognizes the stop codon placed at the suppression site (Figure 2.2 A). Competition for UAA incorporation arises from the protein release factor (RF1 and/or RF2, depending on the stop codon, in prokaryotes and eRF1 in eukaryotes) and recognition of the stop codon results in truncation of the protein, which is typically non-functional, unfolded, and degraded *in vivo* (Figure 2.2 B). Frameshift suppression requires a modified frameshift suppressor tRNA, containing a four-base anticodon, and incorporation of the UAA occurs by suppression at the quadruplet codon (18,25) (Figure 2.2 C). Competition for recognition of the suppression site arises from an endogenous

triplet recognizing tRNA, which causes a –1 frameshift and results in the presentation of an altered amino acid sequence and multiple stop codons (Figure 2.2 D). Another undesired suppression can result when the frameshift suppressor tRNA recognizes a triplet and the adjacent nucleotide (same sequence as the suppression site), resulting in a +1 frameshift. This undesired suppression results in loss of the UAA and results in truncation of the protein (Figure 2.2 E). Due to this undesirable suppression event, mutation of quadruplet codons that are recognized by the frameshift suppressor tRNA can be performed using the degeneracy of the genetic code to increase incorporation efficiency, this is known as “masking” and mutated genes are named the masked constructs (25).

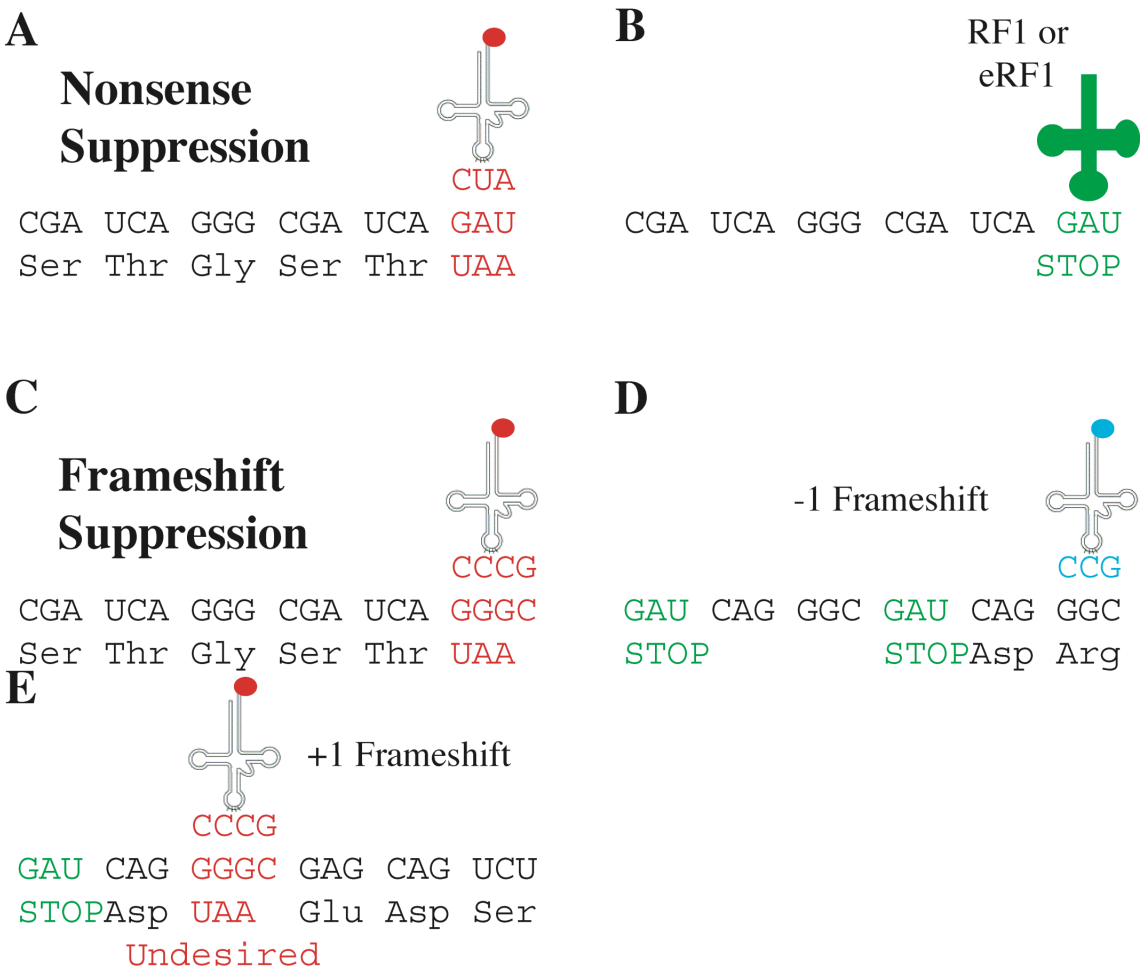

Figure 2.2: Mechanism of nonsense and frameshift suppression. (A) Nonsense suppression, an amber suppressor tRNA recognizes the desired UAG stop codon and incorporates an UAA. (B) Competition for nonsense suppression arises from a protein release factor (RF1, for UAG, in prokaryotes and eRF1 in eukaryotes) and causes termination of the protein sequence. (C) Frameshift suppression, a frameshift suppressor tRNA recognizes the desired four-base codon and incorporates an UAA. The CGGG codon is shown, but any four- or five-base codon is considered frameshift suppression. (D) Competition arises from endogenous tRNA that recognizes the first three bases of the quadruplet codon, which results in a –1 frameshift (at the same position shown in C) and results in truncation by stop codons (shown in green) presented after the -1 frameshift. (E) An undesired suppression event can occur where the frameshift suppressor tRNA recognizes another cognate four-base codon in the mRNA sequence, which results in the incorporation of an UAA and a +1 frameshift. The +1 frameshift causes truncation by stop codons (shown in green) presented after the +1 frameshift. mRNAs are written from 5' to 3' going from right to left. tRNAs are adapted from (1).

The development of frameshift suppression for the *in vivo* incorporation of multiple UAAs was initially analyzed *in vitro* to ensure that the eukaryotic ribosome would tolerate the extended anticodon of the frameshift suppressor tRNAs and/or four-base codons at the suppression site, which was unknown at the start of this research. Initial suppression experiments were performed on the mouse muscle nAChR α-subunit containing an N-terminal hemagglutinin epitope (α_{NHA}), which allows for analysis of truncated and full-length protein by Western blotting (14). The four-base codons analyzed in this study were CGGG (shown to suppress efficiently in previous studies (17,26)), CGUG, and CGUU. CGUG and CGUU were chosen because CGU is the least-used Arg triplet in rabbit (27), which should have less competition with endogenous triplet-recognizing $tRNA^{Arg}$ during translation (Figure 2.2 D) and may increase the suppression efficiency (17,26,28). The human Ser amber suppressor (HSAS) (29), *Tetrahymena thermophila* Gln amber suppressor (THG73) (16), and yeast Phe amber suppressor (YFAS) (18) were used to prepare the frameshift suppressor tRNAs (shown in Figure 2.3). HSAS is aminoacylated by the seryl-tRNA synthetase (SerRS) in mammalian cells (13,29) and was chosen to create frameshift suppressor tRNAs because the *E. coli* SerRS crystal structure reveals no recognition of the anticodon loop (30) and mammalian cells also don't recognize the anticodon (31). THG73 is an orthogonal amber suppressor in *Xenopus* oocytes, in that it is not extensively aminoacylated by the endogenous aminoacyl-tRNA synthetases (aaRSs). THG73 has been used extensively for the incorporation of UAAs (18). YFAS has been modified by the Sisido group and shown to incorporate UAAs by suppressing quadruplet codons (17–19). To create the frameshift suppressor tRNAs, the appropriate anticodons (CCCG, CACG, AACG;

written 5'-3') were placed on HSAS, THG73, and YFAS (Figure 2.3). The frameshift suppressor tRNAs were analyzed *in vitro* by suppressing quadruplet codons in the α_{NHA} and suppression efficiency was evaluated by Western blots and densiometric analysis.

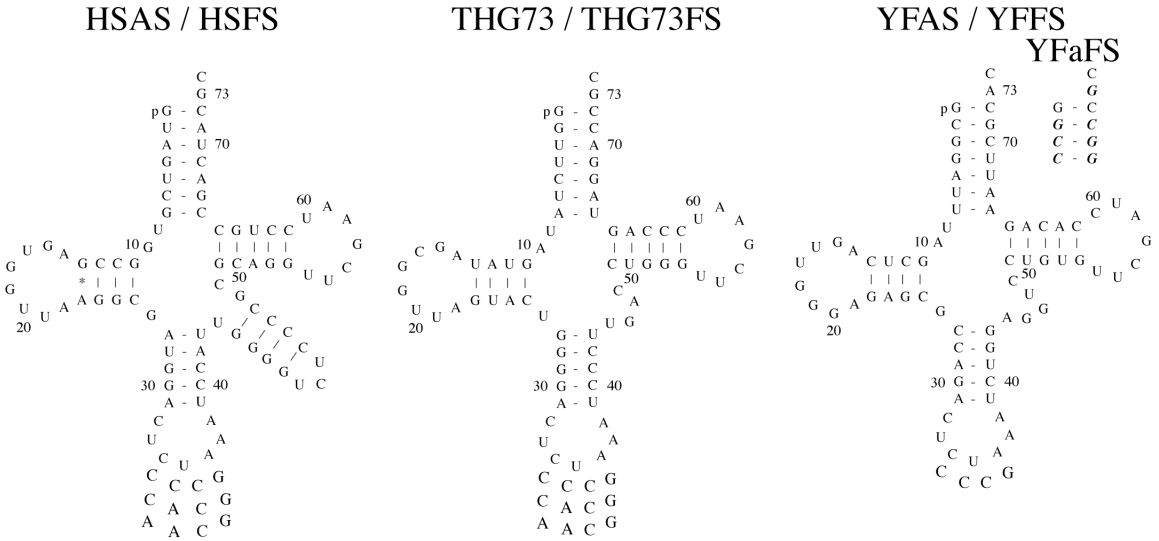

Figure 2.3: Nucleotide sequences and cloverleaf structures of suppressor tRNAs tested *in vitro*. On the left, the human Ser amber suppressor (HSAS) tRNA is shown and is aminoacylated *in vitro* by the SerRS (29). In the middle, *Tetrahymena thermophila* Gln amber suppressor U73G (THG73) is an orthogonal tRNA (not aminoacylated by aaRSs) used for the incorporation of UAAs primarily in *Xenopus* oocytes (16). On the right, the yeast Phe amber suppressor (YFAS) is shown and was the first tRNA used to incorporate UAAs *in vitro* (7). Mutations to the acceptor stem (shown in italics) of the YFAS are shown in the upper right and used by the Sisido group to reduce recognition of frameshift suppressor tRNAs by the GlyRS (19). Below the tRNAs are the four-base anticodons placed on each tRNA to create frameshift suppressor (FS) tRNAs tested *in vitro*.

2.2 Results & Discussion

2.2.1 Experimental Design and Western Blot Analysis

The nAChR α–subunit with the N-terminal HA tag (α_{NHA}) was the initial construct for all mutations because the N-terminal HA tag allows for detection by Western blot (14), all truncations could be visualized, and this was prior to any Arg amino acids that could cause a +1 frameshift (Figure 2.2 E). Initially, constructs were

created at Ser sites because HSAS and HSFS were predicted to be aminoacylated with Ser by the SerRS *in vitro*. Ser154 was chosen as the first suppression site because it was ≈ 1/3 of the protein sequence. Ser374 was chosen as the second suppression site because it was ≈ 2/3 of the protein sequence. These initial suppression sites were thought to be useful for *in vivo* studies later in *Xenopus* oocytes.

The α_{NHA} was translated using rabbit reticulocyte lysate (RRL), nuclease treated *in vitro* reactions unless otherwise noted. Standard Western blotting procedures were followed and done as published (14), unless otherwise noted. The full-length α subunit is predicted to run at 53 KD, but the α-subunit runs on gel as ≈ 45 KD (14). Densiometric analysis was performed using NIH Image, which imports scanned exposures and analyzes the pixel intensity. Bands are manually selected and the average pixel intensity for each band was taken. Suppression efficiency was calculated as written in the Experimental Methods.

2.2.2 HSAS Suppression on α_{NHA}154UAG and α_{NHA}154UAG374UAG

Figure 2.4 shows α_{NHA}154UAG and α_{NHA}154UAG374UAG suppressed with HSAS. The Western blot illustrates that HSAS is aminoacylated in the RRL *in vitro* translation system by an endogenous aaRS, which was previously unknown. The α_{NHA}154UAG construct is suppressed 59% relative to α_{NHA} by 1 μg of HSAS (Figure 2.4, Lane 3), but increased suppression (94%) is seen with 2 μg of HSAS (Figure 2.4, Lane 5). The α_{NHA}154UAG374UAG construct contains two stop codons and requires two suppression events for full-length (FL) protein, and with 2 μg of HSAS the translation efficiency is 33% (Figure 2.4, Lane 7). This illustrates that suppression at two positions is not a concerted event (where suppression of the first UAG facilitates the suppression of

the second UAG), but rather that each suppression is an individual event and the translation efficiency of two sites is equal to the probability of a single suppression event (17). The single suppression efficiency is 59% with 1 μg HSAS and the double translation efficiency is 33% with 2 μg HSAS. The theoretical yield of full-length protein for two suppression events would be equal to 59% X 59% = 35%, which is close to the actual value of 33%. The Western blot in Figure 2.4 is overexposed and the translation efficiencies listed here are actually overestimated.

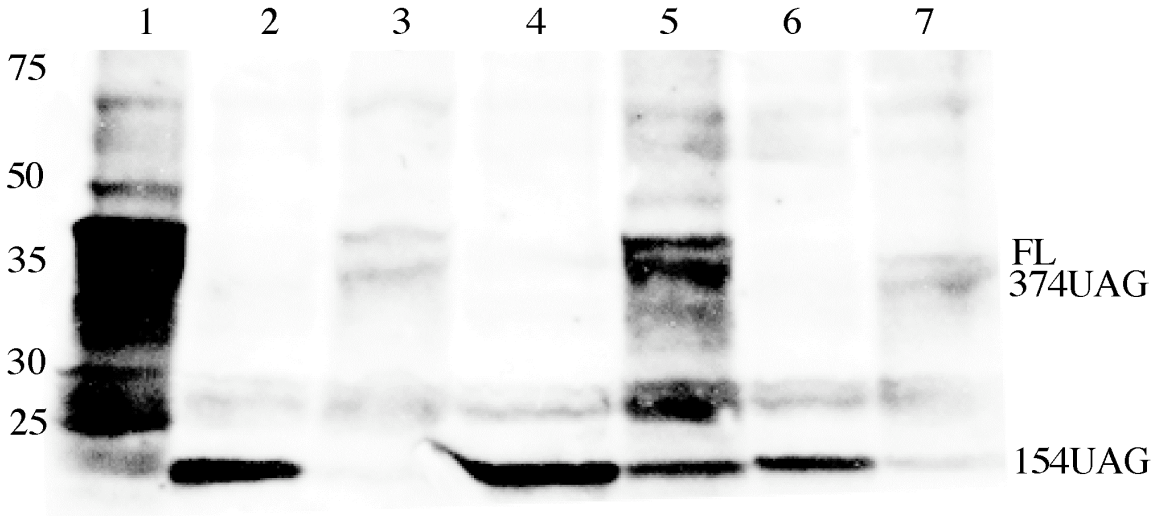

Figure 2.4: HSAS suppression on α_{NHA}154UAG and α_{NHA}154UAG374UAG (2 μg mRNA). Lane 1 shows α_{NHA} and has the highest translation *in vitro*. Lanes 2 and 4, α_{NHA}154UAG mRNA only. Lanes 3 and 5, HSAS suppression on α_{NHA}154UAG with 1 μg and 2 μg of HSAS, respectively. Lane 6, α_{NHA}154UAG374UAG mRNA only. Lane 7, α_{NHA}154UAG374UAG + 2 μg HSAS. Numbers on the left are molecular weight markers (KD). On the right, 154UAG is the first truncation not suppressed by HSAS, 374UAG is the second trunctation after suppression of 154UAG (Lanes 6 and 7 only), and FL is full-length protein band.

2.2.3 HSAS and $HSFS_{CCCG}$ Suppression on α_{NHA}154UAG374CGGG

Figure 2.5 A shows that FL protein with α_{NHA}154UAG374CGGG is dependent on the addition of both HSAS and $HSFS_{CCCG}$, which has a 35% yield of full-length protein

relative to α_{NHA} (Figure 2.5 A, Lane 5). Figure 2.5 B was performed using a RRL coupled *in vitro* translation, where DNA is added and mRNA is transcribed in the system. This Western blot allows for a comparison of two suppression events on α_{NHA}154UAG374CGGG versus one suppression event on α_{NHA}154UAG (Figure 2.5 B). 55% translational efficiency is seen for α_{NHA}154UAG374CGGG with 2 μg of each HSAS and $HSFS_{CCCG}$ (Figure 2.5 B, Lane 4), while α_{NHA}154UAG has a suppression efficiency of 44% with 2 μg of HSAS (Figure 2.5 B, Lane 7). Note efficiencies are exaggerated because the α_{NHA} band is saturated. The α_{NHA}154UAG374CGGG full-length protein yield is also exaggerated due to difficulty in separating the truncation band at 374CGGG and the FL band (Figure 2.5 A, Lane 5, and Figure 2.5 B, Lane 4).

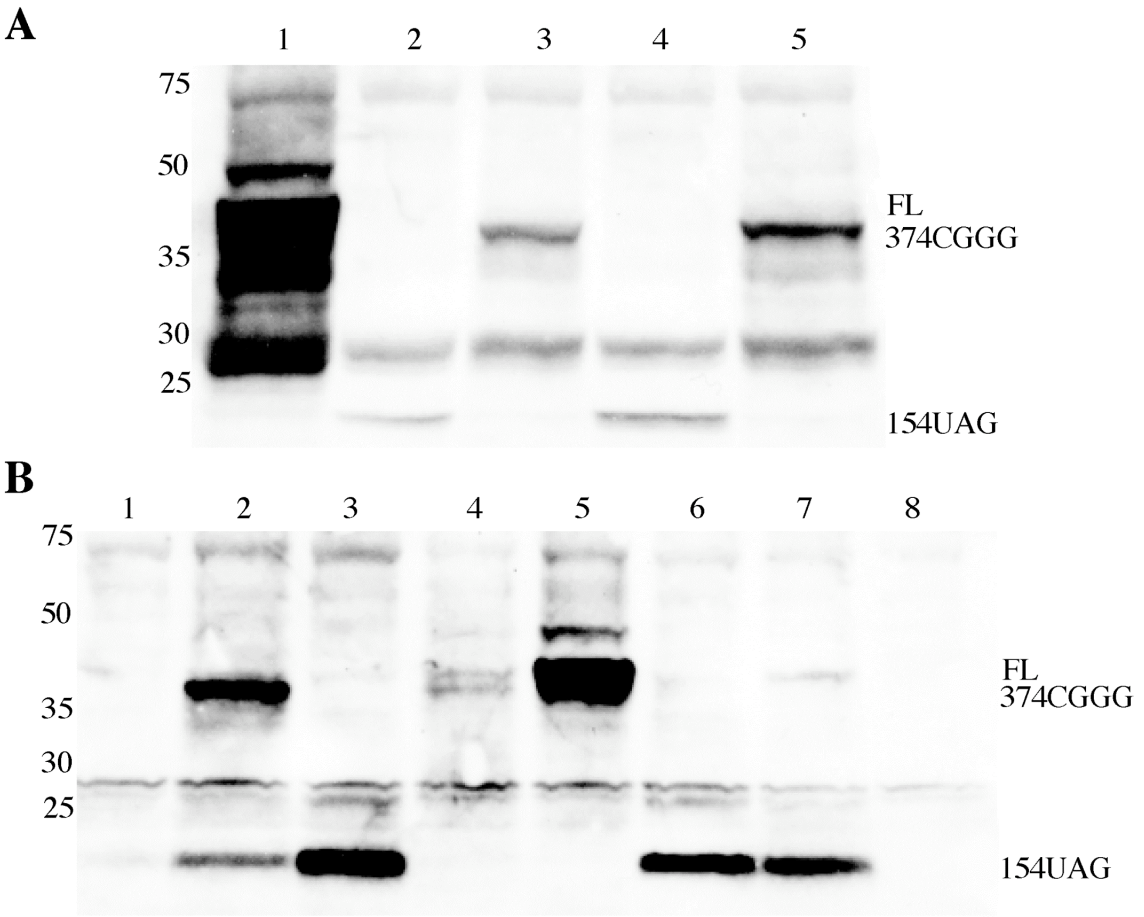

Figure 2.5: HSAS and $HSFS_{CCCG}$ suppression on α_{NHA}154UAG374CGGG. (A) Suppression in RRL with 2 μg mRNA. Lane 1, α_{NHA} mRNA only. Lane 2 is α_{NHA}154UAG374CGGG mRNA only. Lane 3 is α_{NHA}154UAG374CGGG + 2 μg HSAS, which truncates due to the 374CGGG frameshift. Lane 4 is α_{NHA}154UAG374CGGG + 2 μg $HSFS_{CCCG}$ and truncates at 154UAG. Lane 5 is α_{NHA}154UAG374CGGG with 2 μg of HSAS and $HSFS_{CCCG}$. (B) Suppression in TNT RRL with 1 μg DNA. Lanes 1–4 are the same as Lanes 2–5 in part A. Lane 5 is α_{NHA}. Lane 6 is α_{NHA}154UAG mRNA only. Lane 7 is α_{NHA}154UAG + 2 μg of HSAS. Lane 8 is without mRNA and tRNA. Numbers on the left are molecular weight markers (KD). On the right, 154UAG is the first truncation not suppressed by HSAS, 374CGGG is the second trunctation after suppression of 154UAG (not seen for part B Lanes 6–8), and FL is full-length protein band.

At this point in the research, it was determined that frameshift suppression efficiency was too low to proceed with UAAs. Even though HSAS and $HSFS_{CCCG}$ are aminoacylated *in vitro* and should act similarly to endogenous tRNAs, there was not a significant amount of FL protein (Figure 2.5 A, Lane 5, and Figure 2.5 B, Lanes 4 & 7)

compared to the wild-type, α_{NHA} (Figure 2.5 A, Lane 1, and Figure 2.5 B, Lane 5). Also, the 374CGGG truncation was difficult to distinguish from the FL protein (Figure 2.5 A, Lanes 3 & 5, and Figure 2.5 B, Lanes 2 & 4) and an accurate translation efficiency could not be determined. Therefore, single quadruplet codon constructs were created to analyze frameshift suppression accurately and without the dependence of having 154UAG being suppressed prior to the 374CGGG site.

2.2.4 HSAS/HSFS and THG73/THG73FS-Ala Suppression on α_{NHA}154XXX(X)

Figure 2.6 A shows HSAS and HSFS experiments on single suppression constructs at α_{NHA}Ser154XXX(X). α_{NHA}154UAG suppression by HSAS showed suppression efficiency of 49% (Figure 2.6 A, Lane 3), while α_{NHA}154CGGG suppression efficiency by $HSFS_{CCCG}$ was 36% (Figure 2.6 A, Lane 5). The other two quadruplet codons, CGUG and CGUU, show negligible suppression and are within background intensity (Figure 2.6 A, Lanes 6–9). These efficiencies are exaggerated because the α_{NHA} band is saturated (Figure 2.6 A, Lane 1). Figure 2.6 B shows the same experiments as in Figure 2.6 A, but using THG73 and the THG73 frameshift suppressors, which were chemically aminoacylated with Ala. In Figure 2.6 B, no noticeable FL protein is seen for any of the THG73 suppressor tRNAs. Intriguingly the truncated protein band (UAG and four-base codons) was significantly reduced with the addition of tRNA (Figure 2.6 B, Lanes 3, 5, 7 & 9) (reproducible many times). Therefore it is possible that a contaminant may be present within the tRNA samples, even though similar results were continuously seen using newly transcribed tRNA, multiple precipitations with ethanol to remove salt and excess dCA-Ala, and using variable amounts of suppressor tRNA.

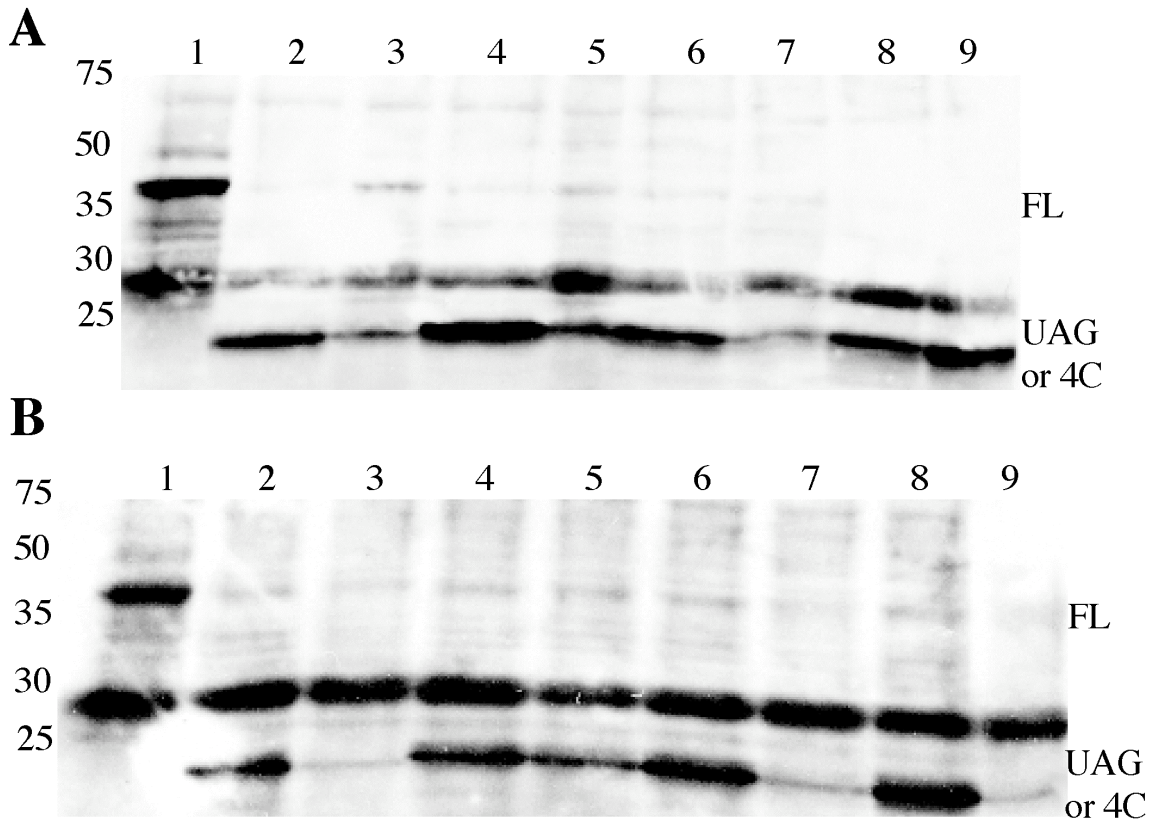

Figure 2.6: HSAS/HSFS and THG73/THG73FS-Ala suppression at α_{NHA}154XXX(X). 1 µg mRNA and 2 µg tRNA were used for both gels. (A) HSAS and HSFS suppression at α_{NHA}154XXX(X). Lane 1 is α_{NHA}. Lane 2 is α_{NHA}154UAG. Lane 3 is α_{NHA}154UAG + HSAS. Lane 4 is α_{NHA}154CGGG. Lane 5 is α_{NHA}154CGGG + $HSFS_{CCCG}$. Lane 6 is α_{NHA}154CGUG. Lane 7 is α_{NHA}154CGUG + $HSFS_{CACG}$. Lane 8 is α_{NHA}154CGUU. Lane 9 is α_{NHA}154CGUU + $HSFS_{AACG}$. (B) THG73-Ala and THG73FS-Ala suppression at α_{NHA}154XXX(X). Lane 1 shows α_{NHA}. Lane 2 is α_{NHA}154UAG. Lane 3 is α_{NHA}154UAG + THG73-Ala. Lane 4 is α_{NHA}154CGGG. Lane 5 is α_{NHA}154CGGG + $THG73FS_{CCCG}$-Ala. Lane 6 is α_{NHA}154CGUG. Lane 7 is α_{NHA}154CGUG + $THG73FS_{CACG}$-Ala. Lane 8 is α_{NHA}154CGUU. Lane 9 is α_{NHA}154CGUU + $THG73FS_{AACG}$-Ala. Numbers on the left are molecular weight markers (KD). On the right, UAG or 4C is the truncation at the stop codon or four-base codon, respectively, and FL is full-length protein band.

The HSFS and THG73FS suppressor tRNAs have not been tested in the literature and are possibly misfolding. Secondary structure of all the tRNAs were predicted using the program mfold to predict nucleic acid folding using standard ionic conditions (32). For HSAS and $HSFS_{CCCG}$ the tRNAs had a similar fold, but were not the native structure shown in Figure 2.3. Interestingly the $HSFS_{CACG}$ and $HSFS_{AACG}$ had the same fold as

HSAS, but in the experiments they were shown to be worse suppressors (Figure 2.6 A). The number of structures for $HSFS_{CACG}$ and $HSFS_{AACG}$ (4 and 5, respectively) is greater than the two structures predicted for HSAS and $HSFS_{CCCG}$. $HSFS_{CACG}$ and $HSFS_{AACG}$ may therefore exist in multiple tertiary structures. THG73 structures were inconclusive because the G-U pair at the base of the anticodon stem (Figure 2.3) is not recognized by mfold. Therefore, the D-loop and the anticodon loop had to be constrained in order to obtain a similar THG73 structure shown in Figure 2.3. $THG73FS_{CCCG}$ and $THG73FS_{CACG}$ showed a similar fold to THG73 with the constraints. $THG73FS_{AACG}$ did not fold properly even with constraints. Structure predictions using mfold are not highly accurate because the overall folding lacks fundamental interactions in a tertiary fold that stabilize the tRNA structure and therefore the folding was inconclusive at determining whether the tRNAs were misfolded by the extended anticodon.

2.2.5 HSAS/HSFS and THG73/THG73FS-Ala Suppression on Single Constructs in Wheat Germ *In Vitro* Translation

Another possibility for loss of protein bands was RNAi, which can occur due to small percentage of antisense tRNA present within a sample (T7 mMessage Machine Transcription kit Ambion manual) or by hybridization of tRNA to the mRNA transcript (RRL Promega manual). Wheat germ extract (WG) for *in vitro* translation of protein is recommended for RNA preparations that may contain low concentrations of dsRNA, which can inhibit the RRL protein translation (WG Promega manual). Figure 2.7 shows the HSAS/HSFS and THG73/THG73FS-Ala suppression experiments (same as Figure 2.6) run in WG reactions. Low translation efficiency of the full-length α_{NHA} protein is seen in both blots. Surprisingly, HSAS suppression on the α_{NHA}154UAG construct shows

more full-length protein than α_{NHA} (Figure 2.7 A, Lane 2). Only small amounts of full-length protein can be seen upon adding HSFS tRNAs (Figure 2.7 A, Lanes 4–9). No full-length protein was seen with THG73/THG73FS-Ala (Figure 2.7 B, Lanes 4–9). Intriguingly, both $HSFS_{CCCG}$ and $THG73FS_{CCCG}$-Ala show a decrease in the truncated product when tRNA is added (Figure 2.7 A & B, Lane 5). α_{NHA}154CGUG also shows a decrease in truncation product when $HSFS_{CACG}$ is added (Figure 2.7 A, Lane 7). This result suggests that RNAi may not be a problematic for the *in vitro* reactions. Therefore, there may be problems with tRNA samples containing a contamination, tRNAs suppressing other sites, and/or tRNAs inhibiting translation. Overall, translation in WG is significantly impaired and yields are not as high as in RRL, which has previously been seen in our lab (Dr. James Petersson and Dr. Niki Zacharias, personal communication).

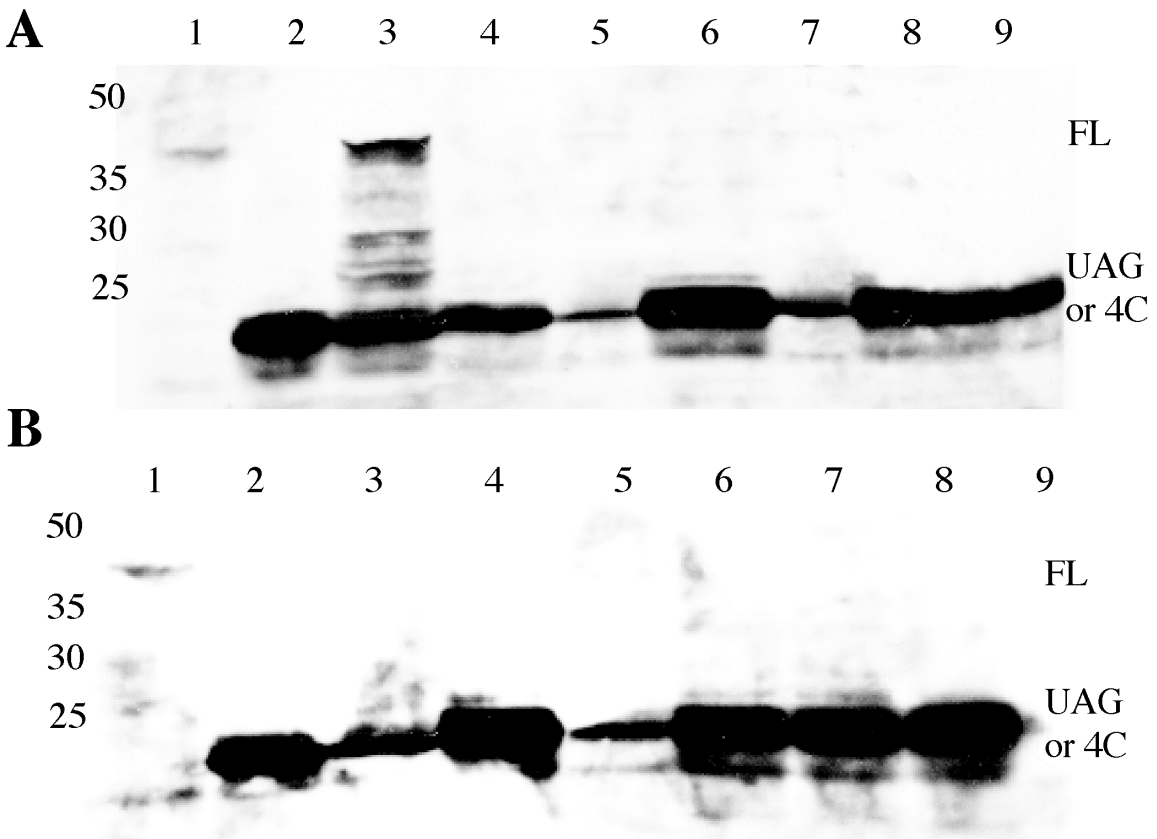

Figure 2.7: HSAS/HSFS and THG73/THG73FS-Ala suppression at α_{NHA}154XXX(X) in wheat germ *in vitro* translation. 1 μg mRNA and 2 μg tRNA (when added) were used for each lane. (A) Lane 1 is α_{NHA}. Lane 2 is α_{NHA}154UAG. Lane 3 is α_{NHA}154UAG + HSAS, which suppresses more efficiently then the translation of α_{NHA} (Lane 1). Lane 4 is α_{NHA}154CGGG and Lane 5 is α_{NHA}154CGGG + $HSFS_{CCCG}$. Lane 6 is α_{NHA}154CGUG and Lane 7 is α_{NHA}154CGUG + $HSFS_{CACG}$. Lane 8 is α_{NHA}15CGUU and Lane 9 is α_{NHA}154CGUU + $HSFS_{AACG}$. (B) Lane 1 is α_{NHA}. Lane 2 is α_{NHA}154UAG. Lane 3 is α_{NHA}154UAG + THG73-Ala. Lane 4 is α_{NHA}154CGGG and Lane 5 is α_{NHA}154CGGG + $THG73FS_{CCCG}$-Ala. Lane 6 is α_{NHA}154CGUG and Lane 7 is α_{NHA}154CGUG + $THG73FS_{CACG}$-Ala. Lane 8 is α_{NHA}15CGUU and Lane 9 is α_{NHA}154CGUU + $THG73FS_{AACG}$-Ala. Both Western blots show little full-length protein for α_{NHA} and translation appears impaired in the wheat germ system. Numbers on the left are molecular weight markers (KD). On the right, UAG or 4C is the truncation at the stop codon or four-base codon, respectively, and FL is full-length protein band.

Another hypothesis was that other sites were being recognized by the FS tRNAs and the reduction in truncated protein was caused by a premature +1 frameshift (Figure 2.2 E). Attempts to detect low molecular weight proteins by Western blot using nitrocellulose and PVDF membranes showed no bands below the 21.3 KD band (data not

shown). This means that there was no truncation present before the α_{NHA}154XXXX suppression site, there is very little truncation of α_{NHA}154XXXX in the sample (undetectable by Coomassie brilliant blue stain; detection limit of 0.1–0.5 μg or Ponceau S staining of the nitrocellulose membrane; detection limit of 1 μg), or the low molecular weight truncations are lost from the membrane during washes for the Western blot procedure.

2.2.6 HSAS/HSFS and THG73/THG73-W Suppression on the α_{NHA}

A new control was then used, which added the FS tRNAs to α_{NHA}. If the FS tRNAs were recognizing different codons, then these would be present on the wild-type α_{NHA} construct and would cause a reduction in the full-length protein band by a +1 frameshift (shown in Figure 2.2 E). Figure 2.8 shows HSFS suppression occurs on α_{NHA} and varies based on the amount of suppressor tRNA added. Figure 2.8 A was an internal control and further testing of the RNAi hypothesis, which should have inhibition of translation with very small amounts of dsRNA. The Western blot (Figure 2.8 A, Lanes 1–4) shows no significant change (< 3%) in full-length protein when 0.1 μg of $HSFS_{CCCG}$, $HSFS_{CACG}$, or $HSFS_{AACG}$ is added, suggesting no inhibition by the RNAi mechanism. However, when 2 μg of FS tRNA is added to α_{NHA} there is a decrease in full-length protein (Figure 2.8 B, Lanes 2–4). $HSFS_{CCCG}$ has a decrease of 38%, $HSFS_{CACG}$ has a decrease of 12%, and $HSFS_{AACG}$ has a decrease of 46% (Figure 2.8 B, Lanes 2–4) relative to α_{NHA} without tRNA (Figure 2.8 B, Lane 1). The difference in reduction in the α_{NHA} suggests that the reduction is not caused by simply the addition of tRNA or by a contaminant (which would be the same for all tRNAs prepared at the same time), but rather suggests a suppression event or events are occurring. Suppression for HSAS on

α_{NHA}154UAG was 60%, $HSFS_{CCCG}$ on α_{NHA}154CGGG was 56%, $HSFS_{CACG}$ on α_{NHA}CGUG was 33%, and $HSFS_{AACG}$ on α_{NHA}CGUU was 43.7% (when compared to α_{NHA}) (Figure 2.8 B, Lanes 5–8). HSAS was only 4.3% more efficient at suppression then $HSFS_{CCCG}$ in this trial. When only 0.1 μg of tRNA was added, suppression efficiency was much higher for HSAS than the HSFS tRNAs, this shows the importance of adding the appropriate amount of tRNA for increased suppression efficiency, which is most likely necessary to out compete endogenous triplet recognizing tRNA (shown in Figure 2.2 D).

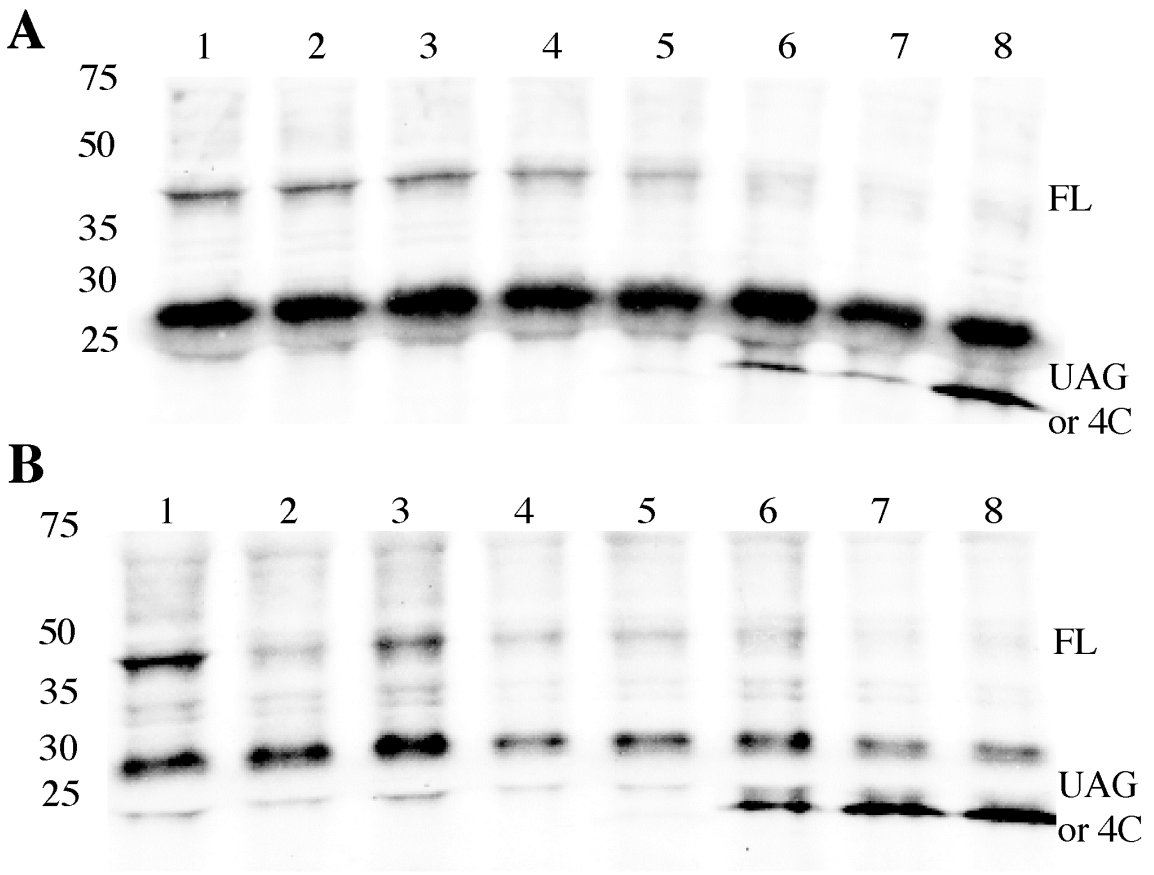

Figure 2.8: HSAS/HSFS suppression on α_{NHA} is dependent on the amount of tRNA added. 2 μg mRNA was used in each reaction. (A) 0.1 μg of HSAS or HSFS tRNA is added in the listed lanes. Lane 1 is α_{NHA}. Lane 2 is α_{NHA} + $HSFS_{CCCG}$. Lane 3 is α_{NHA} + $HSFS_{CACG}$. Lane 4 is α_{NHA} + $HSFS_{AACG}$. Change in full-length protein for α_{NHA} + HSFS tRNAs is < 3% (Lanes 2–4). Lane 5 is α_{NHA}154UAG + HSAS. Lane 6 is α_{NHA}154CGGG + $HSFS_{CCCG}$. Lane 7 is α_{NHA}154CGUG + $HSFS_{CACG}$. Lane 8 is α_{NHA}154CGUU + $HSFS_{AACG}$. (B) 2 μg HSAS or HSFS tRNA was used. Lanes are identical to part A, but with increased amount of tRNA. Full-length α_{NHA} protein is variable when HSFS tRNAs are added (Lanes 2–4) and is different for each tRNA. α_{NHA}154CGGG suppression by $HSFS_{CCCG}$ is comparable to α_{NHA}UAG suppression by HSAS (Lanes 5 & 6). Numbers on the left are molecular weight markers (KD). On the right, UAG or 4C is the truncation at the stop codon or four-base codon, respectively, and FL is full-length protein band.

Figure 2.9 shows representative experiments with HSAS/HSFS and THG73/THG73FS-W tRNAs. HSFS showed similar patterns of reduction on α_{NHA} and suppression on α_{NHA}154XXX(X) as seen in Figure 2.8. However, Figure 2.9 A shows two unknown bands appearing at 29 KD with addition of $HSFS_{CCCG}$ (Figure 2.9 A, Lanes

2 & 6, *) and 22.5 KD for $HSFS_{CACG}$ with α_{NHA}CGUG (Figure 2.9 A, Lane 7). The band at 22.5KD can't be identified based on the Arg triplets in the α_{NHA} and the cause is unknown. The band at 29 KD could possibly be recognition of the Arg182CGG G and the result of a +1 frameshift (Figure 2.2 E). $THG73FS_{CCCG}$-W showed a significant decrease of full-length protein when added to α_{NHA} (Figure 2.9 B, Lane 2), but little full-length protein is seen when added to α_{NHA}154CGGG (Figure 2.9 B, Lane 6). Very little suppression is seen with any of the THG73FS-W tRNAs (Figure 2.9 B, Lanes 6–8).

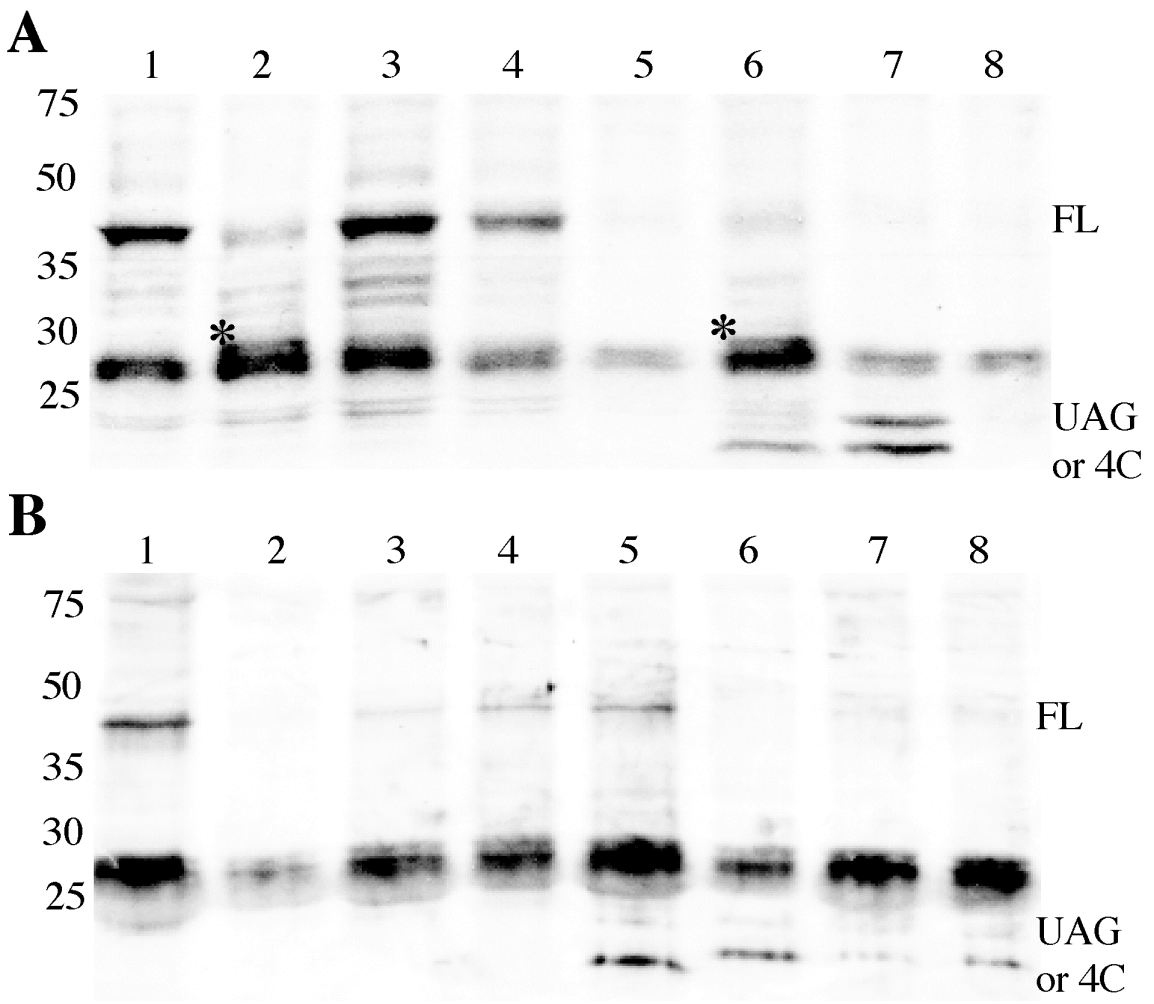

Figure 2.9: HSAS/HSFS and THG73/THG73FS-W suppression on α_{NHA} or α_{NHA}154XXX(X). 4 μg mRNA and 2 μg tRNA are used in both gels. (A) HSAS/HSFS suppression on α_{NHA} (Lanes 2-4) and on α_{NHA}154XXX(X) (Lanes 5–8). Lane 1 is α_{NHA}. Lane 2 is α_{NHA} + $HSFS_{CCCG}$. Lane 3 is α_{NHA} + $HSFS_{CACG}$. Lane 4 is α_{NHA} + $HSFS_{AACG}$. Lane 5 is α_{NHA}154UAG + HSAS. Lane 6 is α_{NHA}154CGGG + $HSFS_{CCCG}$. Lane 7 is α_{NHA}154CGUG + $HSFS_{CACG}$. Lane 8 is α_{NHA}154CGUU + $HSFS_{AACG}$. The * represents a novel band only seen with $HSFS_{CCCG}$ and thought to be caused by a +1 frameshift at R182CGGG (Figure 2.2 E) (Lanes 2 & 6). (B) THG73/THG73FS-W suppression on α_{NHA} (Lanes 2–4) and on α_{NHA}154XXX(X) (Lanes 5–8). Lane 1 is α_{NHA}. Lane 2 is α_{NHA} + $THG73FS_{CCCG}$-W. Lane 3 is α_{NHA} + $THG73FS_{CACG}$-W. Lane 4 is α_{NHA} + $THG73FS_{AACG}$-W. Lane 5 is α_{NHA}154UAG + THG73-W. Lane 6 is α_{NHA}154CGGG + $THG73FS_{CCCG}$-W. Lane 7 is α_{NHA}154CGUG + $THG73FS_{CACG}$-W. Lane 8 is α_{NHA}154CGUU + $THG73FS_{AACG}$-W. Note the novel band seen (* A, Lanes 2 & 6) was not seen in the $THG73FS_{CCCG}$-W reactions. Numbers on the left are molecular weight markers (KD). On the right, UAG or 4C is the truncation at the stop codon or four-base codon, respectively, and FL is full-length protein band.

When looking at the average densiometric analysis of the HSAS/HSFS reduction or suppression trials, a clear pattern arises (Figure 2.10). The reduction in intensity of $HSFS_{CCCG}$ added to α_{NHA} is similar to the increase in intensity of $HSFS_{CCCG}$ added to the α_{NHA}154CGGG, suggesting a single suppression event is occurring on α_{NHA} (Figure 2.10). Addition of $HSFS_{CCCG}$ to α_{NHA} causes a reduction of 32% relative to α_{NHA} intensity without tRNA, or suppression efficiency of 32% for $HSFS_{CCCG}$ on the α_{NHA} construct. When $HSFS_{CCCG}$ is added to the α_{NHA}154CGGG construct, full-length protein can only be attained by one suppression event at the desired suppression site (suppression at two sites would result in a +1 frameshift and lack of full-length protein) and the suppression efficiency is 45%. The truncation bands have about the same average intensity and there is no correlation for suppression efficiency and the intensity of the truncation band (Figure 2.10). Looking at the 28 KD and 70 KD (protein bands from the RRL), the intensity is approximately the same for all the lanes and shows that there is no global change in protein concentration (Figure 2.10). HSAS and $HSFS_{CCCG}$ show the highest suppression efficiency in RRL and amber suppression appears to be better than frameshift suppression with these two tRNAs.

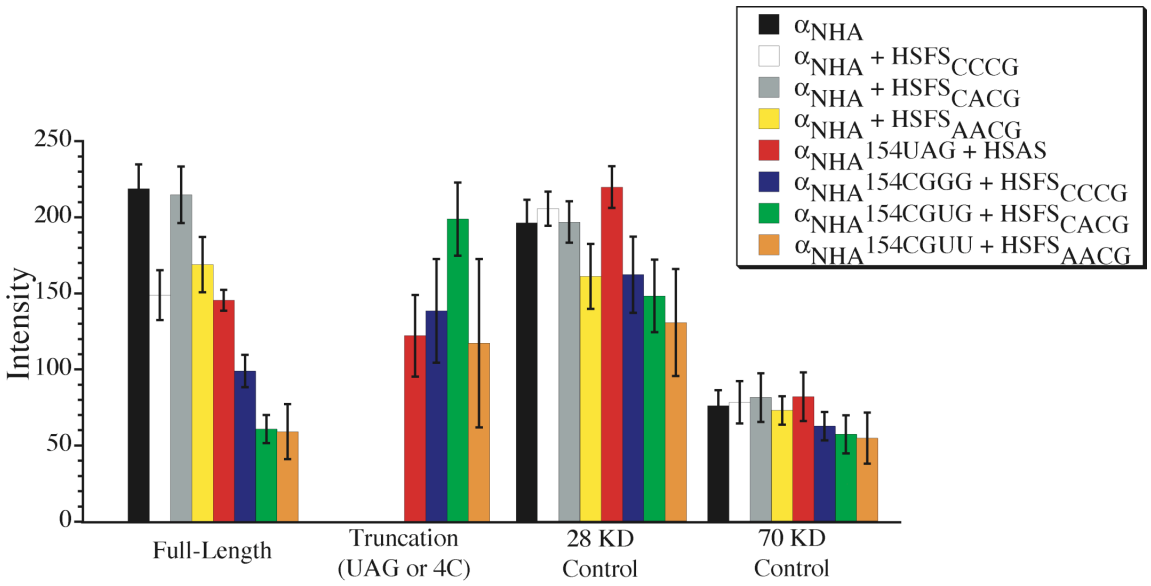

Figure 2.10: Densiometric analysis of HSAS/HSFS suppression on α_{NHA} and α_{NHA}154XXX(X) (average of 6 trials). The α_{NHA} shows the highest intensity of full-length protein, but close to the α_{NHA} + $HSFS_{CACG}$ and suggesting $HSFS_{CACG}$ does not suppress α_{NHA}. α_{NHA} is decreased upon the addition of $HSFS_{CCCG}$ and $HSFS_{AACG}$. The intensity of α_{NHA} + $HSFS_{CCCG}$ is nearly the same as α_{NHA}154UAG + HSAS, suggesting one suppression event is occurring in both cases. α_{NHA}154CGGG + $HSFS_{CCCG}$ shows highest amount of full-length protein for the FS tRNAs. The truncation bands are approximately the same for all tRNAs and show no significant decrease in intensity with increased FL protein. Looking at the 28 KD and 70 KD protein intensities (proteins present in the RRL), there is little difference in these bands between samples and there is no global change in protein concentration.

2.2.7 Arg Mutations, Changing CGG Triplets to CGC Triplets

The previous Western blots (Figure 2.9 A) suggest that the α_{NHA} construct contains a site that is suppressed by $HSFS_{CCCG}$. CGX triplets code for the amino acid Arg and are possible sites for suppression by $HSFS_{CCCG}$. Based on the 29 KD band (Figure 2.9 A, Lanes 2 & 6) and cognate sequence for $HSFS_{CCCG}$ being CGGG, Arg182 was first mutated from CGG to CG*C*. CG*C* was chosen to place the same nucleotide in the mRNA that would be used for recognition by the $HSFS_{CCCG}$ anticodon (5'-C*C*CG-3') and avoid recognition. The Arg mutants were placed in the α_{NHA} and α_{NHA}154CGGG constructs.

These are named by the construct with Arg mutation and the appropriate number following.

Figure 2.11 shows the Western blot of the Arg182 mutants. It was hoped the mutation would lead to a significant increase in the amount of full-length protein in both the α_{NHA}R182 mutant (Figure 2.11, Lane 6) and α_{NHA}154CGGGR182 mutant (Figure 2.11, Lane 4) upon addition of $HSFS_{CCCG}$. α_{NHA}R182 shows higher full-length protein (Figure 2.11, Lane 5) than α_{NHA} (Figure 2.11, Lane 1), most likely because the α_{NHA}R182 mRNA was prepared after the α_{NHA} mRNA. Upon addition of $HSFS_{CCCG}$ to the α_{NHA} and α_{NHA}R182 (Figure 2.11, Lanes 2 & 6) a reduction of 41% and 35%, respectively, was seen when compared to the same mRNA without $HSFS_{CCCG}$. α_{NHA}154UAG suppression by HSAS is either 76% relative to α_{NHA} or 68% relative to α_{NHA}R182 (Figure 2.11, Lane 8). $HSFS_{CCCG}$ suppression of α_{NHA}154CGGGR182 and α_{NHA}154CGGG (Figure 2.11, Lanes 4 & 7, respectively) showed efficiency of 41% and 30%, respectively. The mutation at R182 shows an improvement of 7% at protecting the α_{NHA}R182 from $HSFS_{CCCG}$ suppression (Figure 2.11, Lane 6) and an increase of 11% on the full-length protein for α_{NHA}154CGGGR182 suppressed by $HSFS_{CCCG}$ (Figure 2.11, Lane 4). While this is an improvement, the suppression wasn't increased as much as was hoped and there may be other triplets that are recognized on α_{NHA}.

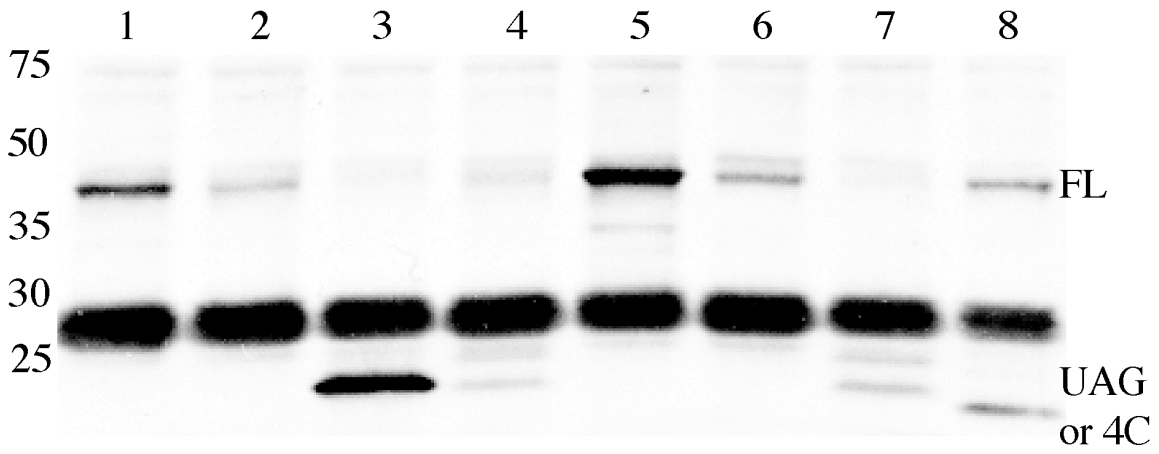

Figure 2.11: $HSFS_{CCCG}$ suppression on α_{NHA}R182 and α_{NHA}154CGGGR182 mutants. 2 μg mRNA and 2 μg tRNA were used for the experiments. Lane 1 is α_{NHA} and Lane 2 is α_{NHA} + $HSFS_{CCCG}$. Lane 3 is α_{NHA}154CGGGR182 and Lane 4 is α_{NHA}154CGGGR182 + $HSFS_{CCCG}$. Lane 5 is α_{NHA}R182 and Lane 6 is α_{NHA}R182 + $HSFS_{CCCG}$. Lane 7 is α_{NHA}154CGGG + $HSFS_{CCCG}$. Lane 8 is α_{NHA}154UAG + HSAS. Numbers on the left are molecular weight markers (KD). On the right, UAG or 4C is the truncation at the stop codon or four-base codon, respectively, and FL is full-length protein band.

Further Arg CGG triplets were mutated to CGC. Arg19 and Arg116 were chosen because they were closer to the N-terminus of the protein and these mutations should cause greater full-length protein or possibly new bands that could be detected on the Western blot. The α_{NHA}154CGGGR19R116 mutation showed a slight increase in suppression when $HSFS_{CCCG}$ was added when compared to α_{NHA}R182 + $HSFS_{CCCG}$. Overall, the α_{NHA}154CGGG constructs with the Arg mutants showed little change in suppression efficiency. Therefore, it appears that only the in-frame CGGG codons need to be removed, such as R182. The R182 is present on the α_{NHA} in all experiments and is known as the "masked" construct (33).

2.2.8 Optimization of the RRL *In Vitro* Reactions for Increased Suppression Efficiencies

In vitro translation reactions are sensitive to organic molecules and salt that is added with the tRNA and mRNA (RRL Promega manual). In order to add more mRNA and tRNA, desalting columns were used. The removal of excess salt and dCA-W from the mRNA transcription and tRNA ligations allowed for greater concentrations of mRNA and tRNA-W in the reactions, which caused increased protein production. The tRNAs are stored at -80 ˚C and this can cause aggregation and unfolding of the tRNA. tRNA was refolded at 65 ˚C for two minutes, as was done for UAA incorporation in *Xenopus* oocytes (8,16). Translation reactions were also allowed to proceed for 3–4 h, rather than 1.5 h. This allowed for increased protein, which was also seen by Dr. James Petersson (personal communication). These changes all helped to increase protein production and were easy to implement.

The most important factor was reducing competition with endogenous triplet recognizing tRNA in order to increase the suppression efficiency of the FS tRNA. The Sisido group performed UAA incorporation in *E. coli in vitro* translation system using 10-fold less Arg in the reaction (34). Removing Arg decreases the competition of the FS tRNAs with endogenous triplet recognizing tRNAs. Therefore, the Arg concentration was reduced 10-fold and this greatly increased the suppression efficiency, as discussed below. Finally, the concentration of tRNA is important for the suppression efficiency. The Sisido group used ≈ 6.8 μg of tRNA-dCA-UAA per 10 μl *E. coli* translation reaction (18). Addition of more tRNA-dCA-UAA also decreases competition with endogenous triplet recognizing tRNA and increased the overall amount of protein. After making

these optimizations, it was very easy to observe and quantify suppression in the RRL *in vitro* reactions.

2.2.9 Choosing a New Frameshift Suppressor tRNA, $YFFS_{CCCG}$

All three of THG73FS showed no suppression in the *in vitro* reactions (Figures 2.6 & 2.9), even though THG73 could suppress the amber codon. At the time, only the yeast Phe frameshift suppressor (YFFS) had been used to incorporate UAAs *in vitro* (18,19,26). $YFFS_{CCCG}$ (sequence shown in Figure 2.3) was chosen as the next suppressor tRNA to be tested because $HSFS_{CCCG}$ worked well in RRL and had been used extensively by the Sisido group.

$YFFS_{CCCG}$-W shows suppression in RRL and is dependent on the amount of tRNA added (Figure 2.12). Figure 2.12, Lanes 2 and 3 show α_{NHA}154CGGG + $YFFS_{CCCG}$-W with 3.4 μg and 6.8 μg, respectively, and show a suppression efficiency of 37% and 46%, respectively. This efficiency exceeded any of the THG73FS-A/W experiments. α_{NHA}154CGGG + $HSFS_{CCCG}$ showed a suppression efficiency of 100% (Figure 2.12, Lane 4) using the optimized conditions. α_{NHA}154UAG + HSAS also had a suppression efficiency of 100% (Figure 2.12, Lane 6), showing that both nonsense and frameshift suppression could be comparable *in vitro* under optimized conditions.

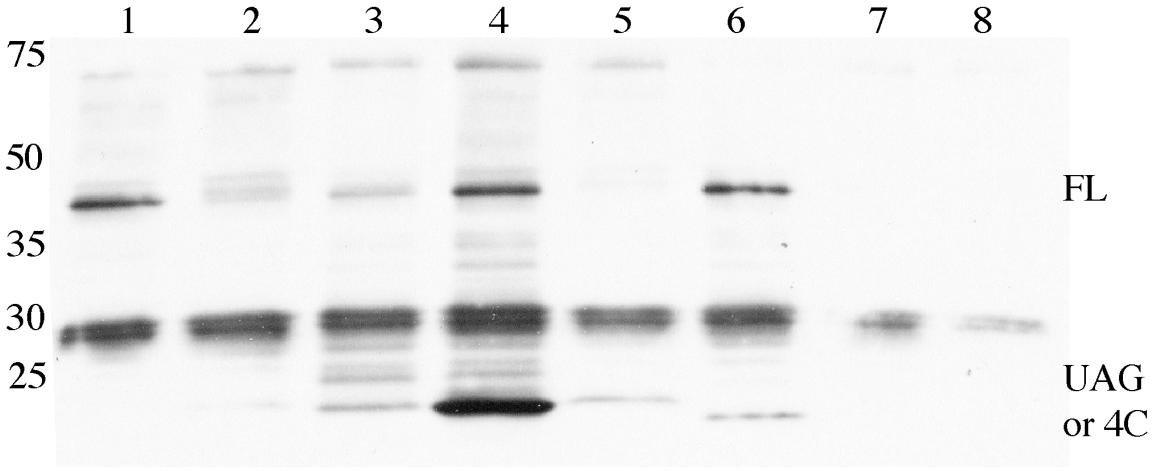

Figure 2.12: $YFFS_{CCCG}$-W and $HSFS_{CCCG}$ suppression at α_{NHA}154XXX(X). 4 μg mRNA were used in each lane. Lane 1 is α_{NHA}. Lane 2 is α_{NHA}154CGGG + 3.4 μg $YFFS_{CCCG}$-W. Lane 3 is α_{NHA}154CGGG + 6.8 μg $YFFS_{CCCG}$-W. Lane 4 is α_{NHA}154CGGG + 5.5 μg $HSFS_{CCCG}$. Lane 5 is α_{NHA}154CGGG. Lane 6 is α_{NHA}154UAG + 5.5 μg HSAS. Lane 7 is α_{NHA}154UAG. Lane 8 is RRL without mRNA and tRNA. Note all constructs contain the R182 mutation and reactions were performed using optimized conditions. Numbers on the left are molecular weight markers (KD). On the right, UAG or 4C is the truncation at the stop codon or four-base codon, respectively, and FL is full-length protein band.

Previously, the Sisido group had shown that the $YFFS_{CCCG}$ can be aminoacylated by endogenous aaRSs in *E. coli in vitro* reactions (19,35). In *E. coli in vitro* reactions, $YFFS_{CCCG}$ is predominately aminoacylated by the ArgRS (35). However, $YFFS_{ACCC}$ is recognized in *E. coli in vitro* reactions by the GlyRS and mutations were made to the acceptor stem (shown in Figure 2.3) to decrease recognition (19). These acceptor stem mutations were made to create $YFaFS_{CCCG}$ (shown in Figure 2.3). The discriminator base (N73) is also an important recognition by many aaRSs in prokaryotic and eukaryotic cells (36,37). Work in *Xenopus* oocytes established that mutation of the discriminator base drastically decreased aminoacylation of THG73 (16). Therefore, A73 of $YFFS_{CCCG}$ was mutated to G73 to create $YFG73FS_{CCCG}$ (shown in Figure 2.3).

Figure 2.13 shows suppression (-Trp) and reaminoacylation experiments with $YFFS_{CCCG}$, $YFG73FS_{CCCG}$, and $YFaFS_{CCCG}$. $YFFS_{CCCG}$-W had a suppression efficiency of

16% (Figure 2.13, Lane 2) and $YFFS_{CCCG}$ (74 mer) had 22% full-length protein of α_{NHA} (Figure 2.13, Lane 3). The suppression efficiency of $YFFS_{CCCG}$-W was not typical. $YFG73FS_{CCCG}$-W showed a suppression efficiency of 60% (Figure 2.13, Lane 4) and $YFG73FS_{CCCG}$ (74 mer) had 24% full-length protein of α_{NHA} (Figure 2.13, Lane 5). $YFFS_{CCCG}$ and $YFG73FS_{CCCG}$ (74 mer) show approximately the same amount of reaminoacylation product (Figure 2.13, Lanes 3 & 5). $YFaFS_{CCCG}$-W had a suppression efficiency of 26% (Figure 2.13, Lane 6), but $YFaFS_{CCCG}$ (74 mer) had 10% full-length protein of α_{NHA} (Figure 2.13, Lane 7). This reaminoacylation is very close to the α_{NHA}154CGGG mRNA only, which had 9% of α_{NHA} (Figure 2.13, Lane 8). $HSFS_{CCCG}$ showed a suppression efficiency of 33% (Figure 2.13, Lane 9). This Western blot shows that reaminoacylation of $YFFS_{CCCG}$ and $YFG73FS_{CCCG}$ can be problematic in the RRL using the optimized conditions.

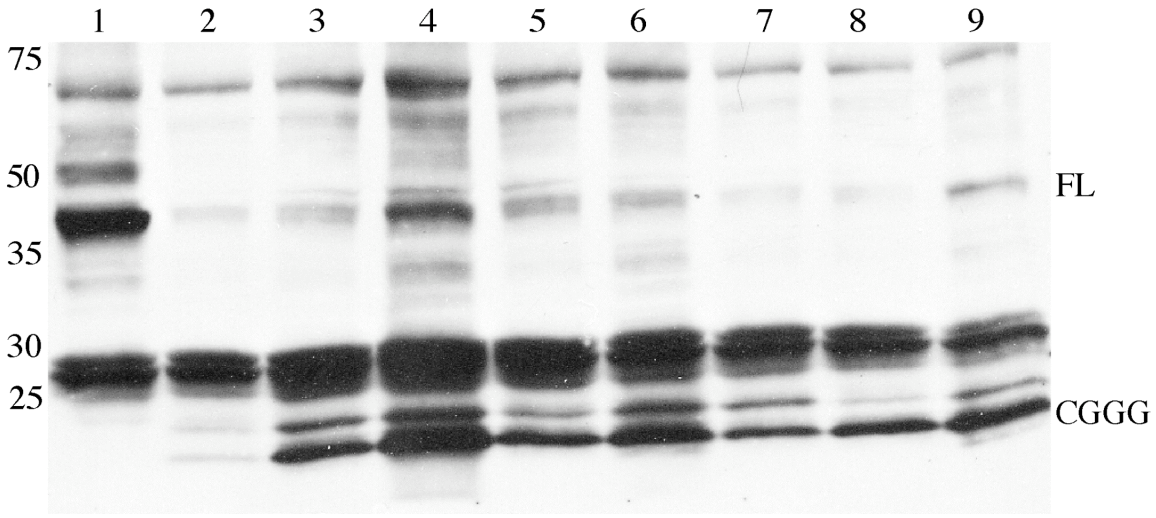

Figure 2.13: $YFFS_{CCCG}$, $YFG73FS_{CCCG}$, $YFaFS_{CCCG}$ (-Trp), and $HSFS_{CCCG}$ suppression and reaminoacylation (74 mer) tested at α_{NHA}154CGGG. 4 μg of mRNA, 6.8 μg of $YFFS_{CCCG}$, $YFG73FS_{CCCG}$, $YFaFS_{CCCG}$ (-W or 74 mer), and 5.5 μg of $HSFS_{CCCG}$ were used in each lane. Lane 1 is α_{NHA}. Lane 2 is α_{NHA}154CGGG + $YFFS_{CCCG}$-W. Lane 3 is α_{NHA}154CGGG + $YFFS_{CCCG}$ (74 mer). Lane 4 is α_{NHA}154CGGG + $YFG73FS_{CCCG}$-W. Lane 5 is α_{NHA}154CGGG + $YFG73FS_{CCCG}$ (74 mer). Lane 6 is α_{NHA}154CGGG + $YFaFS_{CCCG}$-W. Lane 7 is α_{NHA}154CGGG + $YFaFS_{CCCG}$ (74 mer). Lane 8 is α_{NHA}154CGGG. Lane 9 is α_{NHA}154CGGG + $HSFS_{CCCG}$. All constructs contain the R182 mutation and reactions performed using optimized conditions. Numbers on the left are molecular weight markers (KD). On the right, CGGG is the truncation at the four-base codon and FL is full-length protein band.

2.2.10 HSAS and HSFS Suppression at α_{NHA}149XXX(X)

All previous work had been done suppressing at α_{NHA}154XXX(X) and therefore we wanted to look at a second suppression site that would be in a similar location, but also useful for *in vivo* studies. We chose to study α149W of the nAChR because this residue makes a cation-π interaction with acetylcholine and causes a noticeable shift in EC_{50} when fluorinated Trp (UAAs) are incorporated at the site (15). Figure 2.14 shows suppression experiments with HSAS and $HSFS_{CCCG}$ at α_{NHA}154XXX(X) and α_{NHA}149XXX(X) for comparison. $HSFS_{CCCG}$ suppresses comparably at both α_{NHA}154CGGG (Figure 2.14, Lane 2) and α_{NHA}149CGGG (Figure 2.14, Lane 5). HSAS also shows comparable suppression at both sites (Figure 2.14, Lanes 7 & 9). All

suppression was > 100% of α_{NHA}, which appears to not have translated well (Figure 2.14, Lane 1). Most intriguing is that you can see the difference in molecular weight of the truncation bands. The frameshift at α_{NHA}154CGGG is predicted to have a mass of 21.3 KD, α_{NHA}149CGGG is predicted to have a mass of 20.6 KD, α_{NHA}154UAG is predicted to have a mass of 20.4 KD, and α_{NHA}149UAG is predicted to have a mass of 20.2 KD. These were arranged on the Western blot from highest molecular weight (Figure 2.14, Lanes 2 & 3) to lowest molecular weight (Figure 2.14, Lanes 8 & 9). The correlation in migration and predicted mass shows that the frameshift suppression has the correct truncation pattern and is properly truncating in RRL.

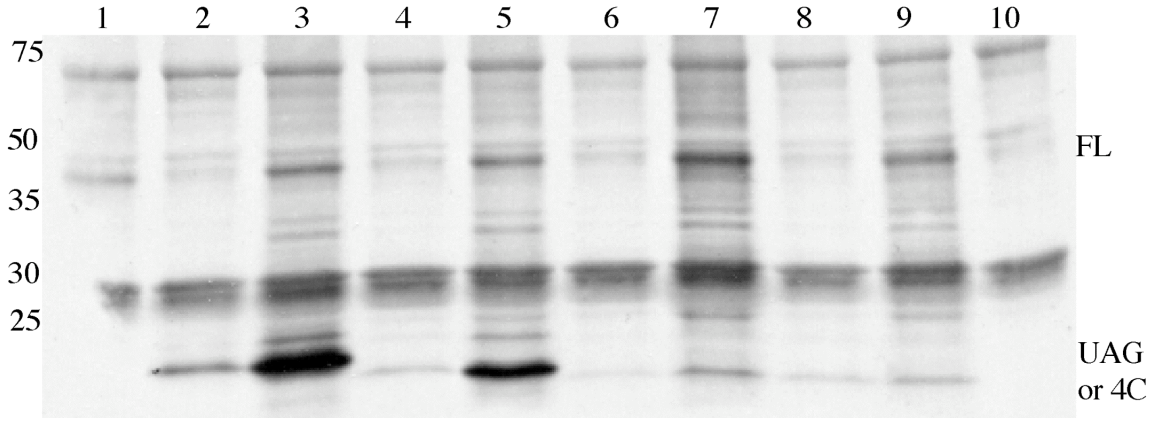

Figure 2.14: $HSFS_{CCCG}$ and HSAS suppression at α_{NHA}154XXX(X) and α_{NHA}149XXX(X). 4 μg of mRNA and 5.5 μg of tRNA were used in each lane. Lane 1 is α_{NHA}. Lane 2 is α_{NHA}154CGGG. Lane 3 is α_{NHA}154CGGG + $HSFS_{CCCG}$. Lane 4 is α_{NHA}149CGGG. Lane 5 is α_{NHA}149CGGG + $HSFS_{CCCG}$. Lane 6 is α_{NHA}154UAG. Lane 7 is α_{NHA}154UAG + HSAS. Lane 8 is α_{NHA}149UAG. Lane 9 is α_{NHA}149UAG + HSAS. Lane 10 is RRL without mRNA and tRNA. All constructs contain the R182 mutation and reactions performed using optimized conditions. Numbers on the left are molecular weight markers (KD). On the right, UAG or 4C is the truncation at the stop codon or four-base codon, respectively, and FL is full-length protein band.

2.2.11 Suppression Efficiencies of Suppressor tRNAs Using Optimized Conditions

After performing Western blots with the optimized conditions and various suppressor tRNAs, the average suppression efficiency relative to α_{NHA}R182 was calculated to allow comparison between different batches of RRL. Figure 2.15 shows the overall suppression efficiency. mRNA only for α_{NHA}154CGGG is 15% and α_{NHA}154UAG is 12% (Figure 2.15, gray bars) and represents the read-through of the suppression site *in vitro* and endogenous protein at the same molecular weight. $HSFS_{CCCG}$ and HSAS suppress almost equivalently with the same amount of tRNA (Figure 2.15, blue bars). Suppression efficiency of the $HSFS_{CCCG}$ is most likely increased because of the decreased concentration of Arg in the *in vitro* reactions, which causes less competition with endogenous triplet recognizing tRNA (Figure 2.2 D). Reaminoacylation of $YFFS_{CCCG}$ (74 mer) occurs in the RRL *in vitro* translation and appears to be increased by the amount of tRNA added and the extended reaction times used under the optimized conditions (Figure 2.15, green bars). Suppression of $YFFS_{CCCG}$-W is also dependent on the amount of tRNA added and increases from 30% to 67% with 3.4 μg to 6.8 μg of $YFFS_{CCCG}$-W, respectively (Figure 2.15, red bars). THG73-W shows an average suppression efficiency of 66%, but only 2 μg of tRNA was used. Overall, frameshift is viable in the RRL *in vitro* system and should work in *Xenopus* oocytes.

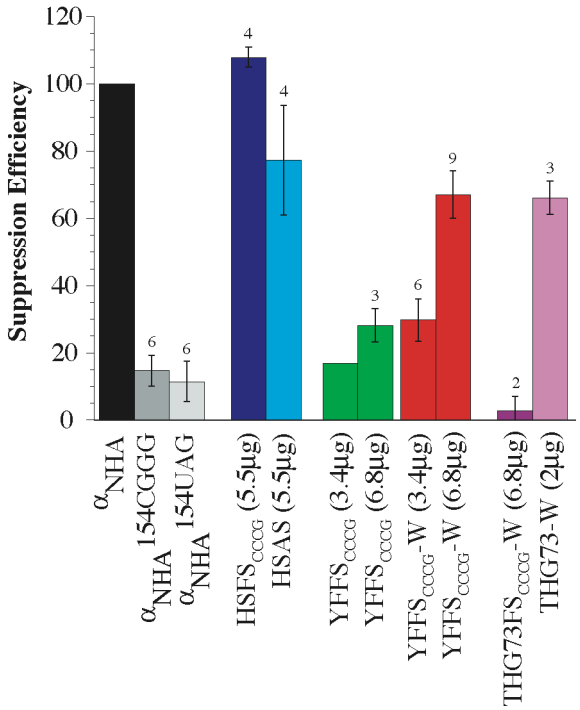

Figure 2.15: Average suppression efficiency and reaminoacylation of suppressor tRNAs using optimized Western blot conditions and α_{NHA}R182. All tRNA were added to their cognate suppression site at α_{NHA}154. α_{NHA}154XXX(X) alone is shown in gray and represents read-through of the protein and endogenous protein at the same molecular weight as the FL protein (background) *in vitro*. The suppression efficiency was expressed relative to α_{NHA}. HSFS$_{CCCG}$ and HSAS show nearly the same suppression efficiency *in vitro* with this amount of tRNA. YFFS$_{CCCG}$ (74 mer) is a reaminoacylation experiment to test if an endogenous aaRS recognizes the tRNA. YFFS$_{CCCG}$-W shows that expression varies with the amount of tRNA added to the RRL. THG73FS$_{CCCG}$-W shows no suppression and the intensity of the full-length band is actually less than the background of α_{NHA}154CGGG alone, which was consistently seen. THG73-W shows approximately the same suppression efficiency as YFFS$_{CCCG}$-W, but there is much less tRNA used for the amber suppressor. Number of Western blot lanes used is listed above each bar, except for α_{NHA}R182, which was always used for normalization, and YFFS$_{CCCG}$ (3.4 µg), which was only performed once.

2.3 Discussion

The eukaryotic *in vitro* translation system described here was invaluable for gaining knowledge about the translational machinery and how the suppressor tRNAs suppress mRNA. RRL appears to be much more efficient in the translation of the nAChR α_{NHA}-subunit than the WG system (Figures 2.6 & 2.7, for direct comparison), which has

been seen by other members of our group (Dr. James Petersson and Dr. Niki Zacharias, personal communication). In order to achieve reproducible protein translation that was much greater than background, it was essential to optimize many components of the mRNA and tRNA handling and purification, reduction of competition for the frameshift suppressors by increasing the amount of tRNA added and decreasing the concentration of Arg, and extending the translation reaction time to 3–4 h. Under these conditions, suppression experiments gave consistent full-length protein intensities that were much stronger than bands with mRNA only (Figures 2.12–2.14). This is necessary to evaluate the suppression efficiency and determine if a suppression event has occurred.

The suppression sites studied here were CGGG, CGUG, and CGUU with both the HSFS and THG73FS tRNAs. CGUG and CGUU were untested at the time the research was performed and show little or no suppression with the HSFS tRNAs in the RRL system. CGGG had been previously used by the Sisido group to incorporate UAAs in *E. coli in vitro* reactions (17,34) and this work showed that CGGG also works in the RRL *in vitro* reactions. After this research was performed, the Sisido group tested multiple quadruplet codons in the RRL system. While CGUG and CGUU were not tested, CGAU showed no suppression efficiency and CGCU showed ≈ 26% suppression efficiency in RRL (21). Therefore it is difficult to predict what quadruplet codons will be suppressible, but the Sisido group has performed many experiments now in *E. coli* and RRL *in vitro* systems to identify functional quadruplet codons (19,21).

HSAS and HSFS tRNAs are exceedingly useful tools for suppression experiments. Both the amber and frameshift suppressor tRNAs are aminoacylated *in vitro* (Figures 2.4–2.9 & 2.11–2.14) and therefore they are useful tools to test suppression

sites without the need to ligate aas or UAAs to the tRNA. Intriguingly, under the optimized conditions there is ≈ 100% suppression efficiency for both HSAS and $HSFS_{CCCG}$ with the same amount of tRNA (Figure 2.15). This suggests that even with the 10-fold reduction in concentration of Arg, competition with endogenous triplet recognizing tRNA with $HSFS_{CCCG}$ (Figure 2.2 D) is comparable to the competition of HSAS with the protein release factor, eRF1 (Figure 2.2 B). The HSAS and HSFS tRNAs can also be compared to tRNA/aminoacyl-tRNA synthetase pairs that have been developed for the incorporation of UAAs *in vivo* (4,11,38). In both cases, the aa or UAA is placed on the tRNA by a protein in the translation reaction and is catalytic. This work establishes that both HSAS and $HSFS_{CCCG}$ are accepted by the translational machinery equally (under the optimum conditions, Figure 2.15) and tRNA/aminoacyl-tRNA synthetase pairs (amber and frameshift) should be extremely useful for *in vitro* translation systems to produce high yields of protein containing multiple UAAs.

THG73 has been used extensively for incorporating UAAs in *Xenopus* oocytes using nonsense suppression at the amber codon (2,3,8,16). However, $THG73FS_{CCCG}$ does not suppress in the *in vitro* translation reactions. Figure 2.9 B, Lane 2 shows a representative reaction where the addition of $THG73FS_{CCCG}$ is added to α_{NHA} (wild-type) and there is virtually no full-length protein produced. When $THG73FS_{CCCG}$ is added to α_{NHA}154CGGG, there is no full-length protein (Figure 2.9 B, Lane 6) and the full-length band shows less intensity than read-through of the mRNA only (Figure 2.15). $THG73FS_{CCCG}$ was not only non-functional, but has a unique phenotype of nearly abolishing translation and/or degrading protein (as determined by the Western blot analysis). Therefore, it is very unlikely that the $THG73FS_{CCCG}$ is simply misfolding or

not accepted by the translational machinery. Rather it is more likely that the tRNA is stalling the ribosome, causing an RNAi response, or some other mechanism that could either stall translation or cause mRNA and/or protein degradation. THG73FS$_{CCCG}$ is unique among the tested suppressor tRNAs for this reason and this information would be unattainable without the use of the *in vitro* system and Western blotting.

The YFFS$_{CCCG}$ was not the original choice for a frameshift suppressor tRNA for the incorporation of UAAs. Previous work had shown that a modified yeast Phe amber suppressor (named MN3) was much less efficient than THG73 at suppressing the amber codon in *Xenopus* oocytes (16). MN3 was also shown to be aminoacylated in the *Xenopus* oocyte greater than THG73 (16). These reaminoacylation experiments were performed at aromatic amino acid sites, which would be the most logical aaRSs that would recognize MN3. YFFS$_{CCCG}$-W was able to suppress in the RRL system (Figures 2.12 & 2.13). After this research was performed, the Sisido group performed research in the RRL system with YFFS$_{CCCG}$-NitroPhe and obtained a suppression efficiency of 64% with 6.8 μg of tRNA suppressing at position 83CGGG of streptavidin (21). This is very close to the suppression efficiency of 68% with YFFS$_{CCCG}$-W (6.8 μg) suppressing at α_{NHA}154CGGG (Figure 2.15). This work therefore agrees with the Sisido group and YFFS$_{CCCG}$ should be useful for the incorporation of UAAs in *Xenopus* oocytes.

Frameshift suppression appears to be unrealistic for use in mammalian cells and other cells that are dividing, because the FS tRNAs would recognize sites on endogenous mRNA, which is suggested by identifying FS tRNAs *in vivo* (28). The recognition of other sites would cause a loss of the UAA and could be toxic to the cell. The *Xenopus* oocyte system is ideal for the use of frameshift suppression because the added mRNA is

predominately translated *in vivo*. Another advantage for the oocyte system is that the most used Arg triplets (AGG and AGA) (27) would not be recognized by the modified FS tRNAs used in this study. Therefore all possible Arg sites could be mutated to either AGG or AGA in the nAChR sequence. This would allow for only competition between the FS tRNAs and endogenous triplet recognizing tRNA at the suppression site. This should increase the total suppression efficiency of the FS tRNAs and may also increase the overall translation efficiency of the nAChR. However, the amount of mutagenesis required to mutate all Arg sites would be time consuming and the Western blots suggest that full-length protein is being produced, which should be detectable by the sensitive assay of electrophysiology.

2.4 Experimental Methods

2.4.1 Materials

Oligonucleotides were synthesized by the California Institute of Technology Biopolymer Synthesis facility. NotI was purchased from Roche Applied Science (Indianapolis). BamHI, EcoRI, FokI, DpnI, MluI, Bsu36I, BstXI, T4 DNA ligase, and T4 RNA ligase were purchased from New England Biolabs (Beverly, MA). Kinase Max, T7 MEGAshortscript, and T7 mMessage mMachine kits were purchased from Ambion (Austin, TX). HA.11 monoclonal antibody from mouse was from Covance (Berkeley, CA). Peroxidase-conjugated affinipure goat anti-mouse IgG was from Jackson Immuno Research (Westgrove, PA).

2.4.2 α_{NHA} Mutations and mRNA Preparation

The α_{NHA} in the pAMV vector was a gift from Dr. Gabriel Brandt. UAG mutations (S154 & S374) and Arg point mutations (CGG to CGC) were made using the QuikChange Site-Directed Mutagenesis (Stratagene). Plasmids were purified using the QIAprep Spin Miniprep Kit (Qiagen), restriction enzyme screened (if possible), and sequenced at the Caltech DNA Sequencing facility.

Four-base codons were mutated by overlap-extension PCR as described (39). Mutagenic PCR primers were ordered with at least 20 base pairs after the mutation region, which consisted of 3 mismatched and 1 insertion for S154 and 5 mismatches and 1 insertion for S374 (extra 2 mismatches to place stop codons). The initial PCR reactions contained 100 ng of DNA template, 1 μg of appropriate outer primer and mutagenic primer, 1 μl 25 mM dNTPs, 5 μl 10X buffer, millipore water to 49 μl, and 1 μl PfuTurbo Hotstart DNA Polymerase (Stratagene). The reaction was run with 30 cycles of 95 ˚C 1 min, 55 ˚C 1 min, and 72 ˚C for 7 min. The reaction mixture was run on a 1% agarose gel and the appropriate length band was purified using QiaQuick Gel Extraction kit (Qiagen). 4 μl of the first two PCR reactions were subjected to another round of PCR using 1 μg of each outer primer. The reaction was run with 30 cycles of 95 ˚C 1 min, 55 ˚C 1 min, and 72 ˚C for 7 min, and the appropriate size band was purified by gel extraction. 25 μl of the PCR product was then digested with MluI and Bsu36I for S154 or Bsu36I and BstXI for S374. Trimmed DNA was gel purified. The trimmed product was subcloned into the trimmed α_{NHA} in the pAMV vector that was dephoshphorylated by shrimp alkaline phosphatase (Boehringer Mannheim Biochemicals) with T4 DNA ligase overnight at 16 ˚C. The ligation reaction was electroporated into bacteria and plasmids

were purified using QIAprep Spin Miniprep Kit (Qiagen), restriction enzyme screened (if possible), and sequenced at the Caltech DNA Sequencing facility.

25–50 μg of mutated DNA was linearized with NotI for 12 h. Linearization was gel screened for completion before extracting with 25:24:1 phenol:chloroform:isoamyl alcohol and precipitated with ethanol for 12 h. DNA was dissolved in 52 μl DEPC water and concentration determined by UV. mRNA was transcribed *in vitro* using T7 mMessage Machine kit for 3–4 h. mRNA was purified using RNeasy kit (Qiagen) and quantified by UV absorption at 260 nm. mRNA was aliquoted and stored at –80 ˚C until used.

2.4.3 Frameshift Suppressor tRNA Gene Construction and tRNA Preparation

HSAS and THG73 tRNA genes in the pUC19 plasmid were a gift from Dr. Sarah Monahan. HSFS tRNAs were made by the following oligonucleotides: 5'-AATTCGTAATACGATCACTATAGTAGTCGTGGCCGAGTGGTTAAGGCGATGGACT(*XXXX*)AATCCATTGGGGTCTCCCCGCGCAGGTTCGAATCCTGCCGACTACGCCATGAGACCCATCCG-3'. THG73FS tRNAs were made by the following oligonucleotides: 5'-AATTCGTAATACGACTCACTATAGGTTCTATAGTATAGCGGTTAGTACTGGGGACT(*XXXX*)AATCCCTTGACCTGGGTTGAATCCCAGTAGGACCGCCAGAGACCCATCCG-3'. XXXX is CCCG, CACG, and AACG (written 5'-3') for both THG73 and HSAS tRNAs. $YFFS_{CCCG}$ was prepared with the following oligonucleotides: 5'-AATTCGTAATACGACTCACTATAGCGGATTTAGCTCAGTTGGGAGAGCGCCAGACT(CCCG)AATCTGGAGGTCCTGTGTTCGATCCACAGAATTCGCACCATGAGACCCATCCG-3'. Note, oligonucleotides contain overlapping ends for ligation into pUC19 with EcoRI and BamHI.

The oligonucleotides were phosphorylated using Kinase Max kit, annealed, ligated to pUC19 plasmid (linearized with EcoRI and BamHI, dephosphorylated with shrimp alkaline phosphatase, purified by gel, and extracted using QiaQuick Gel Extraction kit (Qiagen)) with T4 DNA ligase at 16 ˚C for 12 h. Bacteria were electroporated, plasmids were purified using QIAprep Spin Miniprep Kit (Qiagen), restriction enzyme screened for insert with EcoRI and BamHI, and sequenced at the Caltech DNA Sequencing facility. tRNA were prepared similarly to procedures previously described (16,40).

25–50 μg DNA was linearized with Fok1 for 12 h. The linearization was gel screened for completion before extracting with 25:24:1 phenol:chloroform:isoamyl alcohol and precipitation with ethanol for 12 h. DNA was dissolved in 52 μl DEPC water and concentration determined by UV absorption at 260 nm. tRNA was transcribed *in vitro* using T7-MEGAshortscript kit for 3–4 h, which creates a 74mer tRNA lacking the last two nucleotides. The tRNA was extracted with 25:24:1 phenol:chloroform:isoamyl alcohol and precipitated with isopropanol for 12 h. tRNA was dissolved in DEPC water, run on gel with a previously prepared tRNA sample, quantified by UV absorption at 260 nm, and verified as the correct mass using MALDI-TOF mass spectrometry as described for THG73 (41). Using optimized conditions, the tRNA was dissolved in RNAse free water and desalted using CHROMA SPIN™-30 DEPC-H_2O columns (BD Biosciences, San Jose, CA). tRNA was aliquoted and stored at –80 ˚C until used.

2.4.4 dCA-aa Synthesis and Ligation to Supressor tRNAs

The synthesis of dCA and the coupling of UAAs has been described previously (40,42). dCA-Ala was a gift from Amy Eastwood and dCA-Trp was a gift from Dr. Sarah Monahan. Ligation to THG73, THG73FS, and YFFS tRNAs was performed as previously described (40,41). Briefly, the tRNA is denatured by placing in boiling water and allowed to cool in an ice bath to ≈ 37 ˚C to refold the tRNA. The tRNA is ligated to the dCA-aa using T4 RNA ligase for 30 min (longer times result in increased hydrolysis of the aa). The reaction is then extracted using 25:24:1 phenol:chloroform:isoamyl alcohol at pH = 5.2 and precipitated with ethanol for 12 h (longer precipitation times can result in hydrolysis of the aa). The tRNA was resuspended in DEPC ≈ 1 μg / μl. Using optimized conditions, the tRNA was resuspended in RNAse-free water and desalted using CHROMA SPIN™-30 DEPC-H_2O columns (BD Biosciences, San Jose, CA). The tRNA-dCA-aa was aliquoted and placed at -80 ˚C until used. Ligation efficiency was qualitatively determined by MALDI-TOF as previously described (41).

2.4.5 *In Vitro* Translation

The tRNA was normalized and more concentrated samples were diluted with DEPC water so the same amount of tRNA was added to each *in vitro* reaction. The same was done for the mRNA samples.

Rabbit reticulocyte lysate (RRL), nuclease treated (Promega), was thawed slowly on ice. All reactions on a gel were run with the same tube of RRL. For eight samples, 3/5 reactions were run as follows: 22 μl RRL, 0.9 μl 1 mM aa mix, 0.6 μl RNAse Inhibitor (Roche), various amounts of mRNA and/or tRNA (noted with each figure), and filled to 30 μl with DEPC water. The NVOC protecting group was removed immediately

before use in *in vitro* reactions by irradiation of the tRNA-dCA-aa-NVOC for 5 min with a 1,000 W Hg(Xe) arc lamp as described (40). Translation was run at 30 ˚C for 1.5 h and placed at –80 ˚C. TNT Coupled Reticulocyte Lysate (Promega) was employed the same as RRL with DNA, following manufacturers protocol. The reaction was run for 1.5 h and placed at –80 ˚C.

Wheat germ extract (WG) (Promega) was thawed on ice and all reactions were performed with the same WG tube. 3/5 reactions were performed as follows: 15 μl WG, 1.33 μl 1 mM aa mix, 3.6 μl 1 M KOAc, 1 μl RNAse Inhibitor (Roche), various amounts of mRNA and/or tRNA, and filled to 30 μl with DEPC water. Translation was run at 25 ˚C for 1.5 h and placed at –80 ˚C.

Under optimized conditions, the RRL reaction was performed as follows. For eight samples, 3/5 reactions were run as follows: 22 μl RRL, 1 μl 1 mM 19 aa mix (-Arg), 1 μl 0.1 mM Arg, 0.6 μl RNAse Inhibitor (Roche), various amounts of mRNA and/or tRNA (noted with each figure and greater than un-optimized conditions), and filled to 30 μl with RNase free water. The tRNA was refolding at 65 ˚C for 2 min and the NVOC protecting group was removed immediately before use in *in vitro* reactions by irradiation of the tRNA-dCA-aa-NVOC for 5 min with a 1,000 W Hg(Xe) arc lamp as described (40). Translation was run at 30 ˚C for 3–4 h and placed at –80 ˚C.

2.4.6 Western Blotting and Densiometric Analysis

Western blotting was performed as previously described (14). Briefly 5 μl of crude *in vitro* translation was added to 5 μl of 2X SDS loading buffer. Samples were loaded on a 4–15% linear gradient ready gel Tris-HCl (Bio-Rad) and run at 150 V for 1.25 h or until the hemoglobin (red band from RRL) had run off the gel. Protein was

transferred to nitrocellulose (Bio-Rad) at 30 V for 30 min and 100 V for 1.5 h. Nitrocellulose was blocked for 1 h or overnight using non-fat dairy milk (NFDM) in 1X PBS / 0.1% Tween, placed in 62.5–87.5 μg 1° Ab anti-hemagglutinin (Covance) in 15 ml NFDM / 1X PBS / 0.1% Tween for 1 h, washed 4X with 30 ml 1X PBS / 0.1% Tween for 5 min each, placed in 4 μg Peroxidase-conjugated AffiniPure Goat Anti-Mouse IgG (Jackson ImmunoResearch) in 30 mL NFDM / 1X PBS / 0.1% Tween for 1 h, and washed 4X with 30 ml 1X PBS / 0.1% Tween for 5 min each. Nitrocellulose was visualized using ECL Detection Kit and Hyperfilm ECL (Amersham Biosciences). ECL reagents were left on nitrocellulose for 1 min and quickly exposed for 30 sec, 15 sec, 10 sec, and 5 sec during the highest intensity light emission (1–5 min after exposure to ECL reagents, *Amersham Biosciences manual*).

Densiometric analysis was performed using the NIH Image program (National Institute of Health). Calculation of band intensity was performed similar to the manner of Sisido and coworkers (34). A calibration curve could not be generated because the protein is present in a very small amount, so numbers are qualitative rather than quantitative. Background intensity was determined by various endogenous protein bands in the RRL. Intensities of protein bands reported here are average values across the entire lane. Translation (for two suppression site constructs) or suppression efficiency is calculated by [(Suppressed FL Protein Intensity)/(Wild-type FL Protein Intensity(or similar control))]*100 or for suppression of the wild-type constructs; [1-(Wild-type + tRNA FL Intensity)/(Wild-type FL Intensity)]*100.

2.5 References

1. Link, A.J., Mock, M.L., and Tirrell, D.A. (2003) Non-canonical amino acids in protein engineering. *Curr. Opin. Biotechnol.*, **14**, 603–609.
2. Dougherty, D.A. (2000) Unnatural amino acids as probes of protein structure and function. *Curr. Opin. Biotechnol.*, **4**, 645–652.
3. Beene, D.L., Dougherty, D.A., and Lester, H.A. (2003) Unnatural amino acid mutagenesis in mapping ion channel function. *Curr. Opin. Neurobiol.*, **13**, 264–270.
4. Xie, J., and Schultz, P.G. (2005) An expanding genetic code. *Methods*, **36**, 227–238.
5. Zhang, Z., Alfonta, L., Tian, F., Bursulaya, B., Uryu, S., King, D.S., and Schultz, P.G. (2004) Selective incorporation of 5-hydroxytryptophan into proteins in mammalian cells. *Proc. Natl. Acad. Sci. USA*, **101**, 8882–8887.
6. Rodriguez, E.A., Lester, H.A., and Dougherty, D.A. (2007) Improved amber and opal suppressor tRNAs for incorporation of unnatural amino acids *in vivo*. Part 2: Evaluating suppression efficiency. *RNA*, **13**, 1715–1722.
7. Noren, C.J., Anthonycahill, S.J., Griffith, M.C., and Schultz, P.G. (1989) A general method for site-specific incorporation of unnatural amino acids into proteins. *Science*, **244**, 182–188.
8. Nowak, M.W., Kearney, P.C., Sampson, J.R., Saks, M.E., Labarca, C.G., Silverman, S.K., Zhong, W., Thorson, J., Abelson, J.N., Davidson, N. *et al.* (1995) Nicotinic receptor binding site probed with unnatural amino acid incorporation in intact cells. *Science*, **268**, 439–442.

9. Heckler, T.G., Chang, L.H., Zama, Y., Naka, T., Chorghade, M.S., and Hecht, S.M. (1984) T4 RNA ligase mediated preparation of novel "chemically misacylated" $tRNA^{Phe}$s. *Biochemistry*, **23**, 1468–1473.

10. Wang, L., Magliery, T.J., Liu, D.R., and Schultz, P.G. (2000) A new functional suppressor tRNA/aminoacyl-tRNA synthetase pair for the *in vivo* incorporation of unnatural amino acids into proteins. *J. Am. Chem. Soc.*, **122**, 5010–5011.

11. Chin, J.W., Cropp, T.A., Anderson, J.C., Mukherji, M., Zhang, Z., and Schultz, P.G. (2003) An expanded eukaryotic genetic code. *Science*, **301**, 964–967.

12. England, P.M. (2004) Unnatural amino acid mutagenesis: a precise tool for probing protein structure and function. *Biochemistry*, **43**, 11623–11629.

13. Monahan, S.L., Lester, H.A., and Dougherty, D.A. (2003) Site-specific incorporation of unnatural amino acids into receptors expressed in mammalian cells. *Chem. Biol.*, **10**, 573–580.

14. England, P.M., Zhang, Y.N., Dougherty, D.A., and Lester, H.A. (1999) Backbone mutations in transmembrane domains of a ligand-gated ion channel: Implications for the mechanism of gating. *Cell*, **96**, 89–98.

15. Zhong, W., Gallivan, J.P., Zhang, Y., Li, L., Lester, H.A., and Dougherty, D.A. (1998) From ab initio quantum mechanics to molecular neurobiology: A cation-π binding site in the nicotinic receptor. *Proc. Natl. Acad. Sci. USA*, **95**, 12088–12093.

16. Saks, M.E., Sampson, J.R., Nowak, M.W., Kearney, P.C., Du, F.Y., Abelson, J.N., Lester, H.A., and Dougherty, D.A. (1996) An engineered *Tetrahymena*

tRNA^{Gln} for *in vivo* incorporation of unnatural amino acids into proteins by nonsense suppression. *J. Biol. Chem.*, **271**, 23169–23175.

17. Hohsaka, T., Ashizuka, Y., Sasaki, H., Murakami, H., and Sisido, M. (1999) Incorporation of two different nonnatural amino acids independently into a single protein through extension of the genetic code. *J. Am. Chem. Soc.*, **121**, 12194–12195.

18. Hohsaka, T., Ashizuka, Y., Murakami, H., and Sisido, M. (1996) Incorporation of nonnatural amino acids into streptavidin through *in vitro* frame-shift suppression. *J. Am. Chem. Soc.*, **118**, 9778–9779.

19. Hohsaka, T., Ashizuka, Y., Taira, H., Murakami, H., and Sisido, M. (2001) Incorporation of nonnatural amino acids into proteins by using various four-base codons in an *Escherichia coli in vitro* translation system. *Biochemistry*, **40**, 11060–11064.

20. Hohsaka, T., Fukushima, M., and Sisido, M. (2002) Nonnatural mutagenesis in *E. coli* and rabbit reticulocyte lysates by using four-base codons. *Nucleic Acids Res. Suppl.*, 201–202.

21. Taira, H., Fukushima, M., Hohsaka, T., and Sisido, M. (2005) Four-base codon-mediated incorporation of non-natural amino acids into proteins in a eukaryotic cell-free translation system. *J. Biosci. Bioeng.*, **99**, 473–476.

22. Hohsaka, T., Ashizuka, Y., Murakami, H., and Sisido, M. (2001) Five-base codons for incorporation of nonnatural amino acids into proteins. *Nucleic Acids Res.*, **29**, 3646–3651.

23. Anderson, R.D., 3rd, Zhou, J., and Hecht, S.M. (2002) Fluorescence resonance energy transfer between unnatural amino acids in a structurally modified dihydrofolate reductase. *J. Am. Chem. Soc.*, **124**, 9674–9675.

24. Taki, M., Hohsaka, T., Murakami, H., Taira, K., and Sisido, M. (2002) Position-specific incorporation of a fluorophore-quencher pair into a single streptavidin through orthogonal four-base codon/anticodon pairs. *J. Am. Chem. Soc.*, **124**, 14586–14590.

25. Murakami, H., Kourouklis, D., and Suga, H. (2003) Using a solid-phase ribozyme aminoacylation system to reprogram the genetic code. *Chem. Biol.*, **10**, 1077–1084.

26. Murakami, H., Hohsaka, T., Ashizuka, Y., and Sisido, M. (1998) Site-directed incorporation of *p*-nitrophenylalanine into streptavidin and site-to-site photoinduced electron transfer from a pyrenyl group to a nitrophenyl group on the protein framework. *J. Am. Chem. Soc.*, **120**, 7520–7529.

27. Nakamura, Y., Gojobori, T., and Ikemura, T. (2000) Codon usage tabulated from international DNA sequence databases: Status for the year 2000. *Nucleic Acids Res.*, **28**, 292.

28. Magliery, T.J., Anderson, J.C., and Schultz, P.G. (2001) Expanding the genetic code: Selection of efficient suppressors of four-base codons and identification of "shifty" four-base codons with a library approach in *Escherichia coli*. *J. Mol. Biol.*, **307**, 755–769.

29. Capone, J.P., Sharp, P.A., and RajBhandary, U.L. (1985) Amber, ochre and opal suppressor tRNA genes derived from a human serine tRNA gene. *Embo. J.*, **4**, 213–221.

30. Price, S., Cusack, S., Borel, F., Berthet-Colominas, C., and Leberman, R. (1993) Crystallization of the seryl-tRNA synthetase:$tRNA^{ser}$ complex of *Escherichia coli*. *FEBS Lett.*, **324**, 167–170.

31. Shimada, N., Suzuki, T., and Watanabe, K. (2001) Dual mode recognition of two isoacceptor tRNAs by mammalian mitochondrial seryl-tRNA synthetase. *J. Biol. Chem.*, **276**, 46770–46778.

32. Zuker, M. (2003) Mfold web server for nucleic acid folding and hybridization prediction. *Nucleic Acids Res.*, **31**, 3406–3415.

33. Rodriguez, E.A., Lester, H.A., and Dougherty, D.A. (2006) *In vivo* incorporation of multiple unnatural amino acids through nonsense and frameshift suppression. *Proc. Natl. Acad. Sci. USA*, **103**, 8650–8655.

34. Hohsaka, T., Kajihara, D., Ashizuka, Y., Murakami, H., and Sisido, M. (1999) Efficient incorporation of nonnatural amino acids with large aromatic groups into streptavidin in *in vitro* protein synthesizing systems. *J. Am. Chem. Soc.*, **121**, 34–40.

35. Nakata, H., Ohtsuki, T., Abe, R., Hohsaka, T., and Sisido, M. (2006) Binding efficiency of elongation factor Tu to tRNAs charged with nonnatural fluorescent amino acids. *Anal. Biochem.*, **348**, 321–323.

36. Giege, R., Sissler, M., and Florentz, C. (1998) Universal rules and idiosyncratic features in tRNA identity. *Nucleic Acids Res.*, **26**, 5017–5035.

37. Saks, M.E., Sampson, J.R., and Abelson, J.N. (1994) The transfer RNA identity problem: A search for rules. *Science*, **263**, 191–197.

38. Deiters, A., Cropp, T.A., Mukherji, M., Chin, J.W., Anderson, J.C., and Schultz, P.G. (2003) Adding amino acids with novel reactivity to the genetic code of *Saccharomyces cerevisiae*. *J. Am. Chem. Soc.*, **125**, 11782–11783.

39. Ling, M.M., and Robinson, B.H. (1997) Approaches to DNA mutagenesis: an overview. *Anal. Biochem.*, **254**, 157–178.

40. Nowak, M.W., Gallivan, J.P., Silverman, S.K., Labarca, C.G., Dougherty, D.A., and Lester, H.A. (1998) *In vivo* incorporation of unnatural amino acids into ion channels in *Xenopus* oocyte expression system. *Meth. Enzymol.*, **293**, 504–529.

41. Petersson, E.J., Shahgholi, M., Lester, H.A., and Dougherty, D.A. (2002) MALDI-TOF mass spectrometry methods for evaluation of *in vitro* aminoacyl tRNA production. *RNA*, **8**, 542–547.

42. Robertson, S.A., Noren, C.J., Anthony-Cahill, S.J., Griffith, M.C., and Schultz, P.G. (1989) The use of 5'-phospho-2 deoxyribocytidylylriboadenosine as a facile route to chemical aminoacylation of tRNA. *Nucleic Acids Res.*, **17**, 9649–9660.